

# Journal Pre-proof

Design, synthesis, and *in vitro* and *in vivo* anti-angiogenesis study of a novel vascular endothelial growth factor receptor-2 (VEGFR-2) inhibitor based on 1,2,3-triazole scaffold

De-pu Wang, Kai-li Liu, Xin-yang Li, Guo-qing Lu, Wen-han Xue, Xin-hua Qian, Kamara Mohamed O, Fan-hao Meng

PII: S0223-5234(20)31055-2

DOI: <https://doi.org/10.1016/j.ejmech.2020.113083>

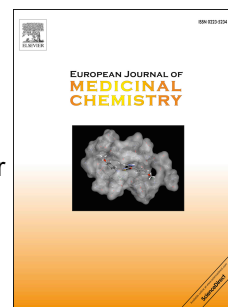
Reference: EJMECH 113083

To appear in: *European Journal of Medicinal Chemistry*

Received Date: 31 August 2020

Revised Date: 1 December 2020

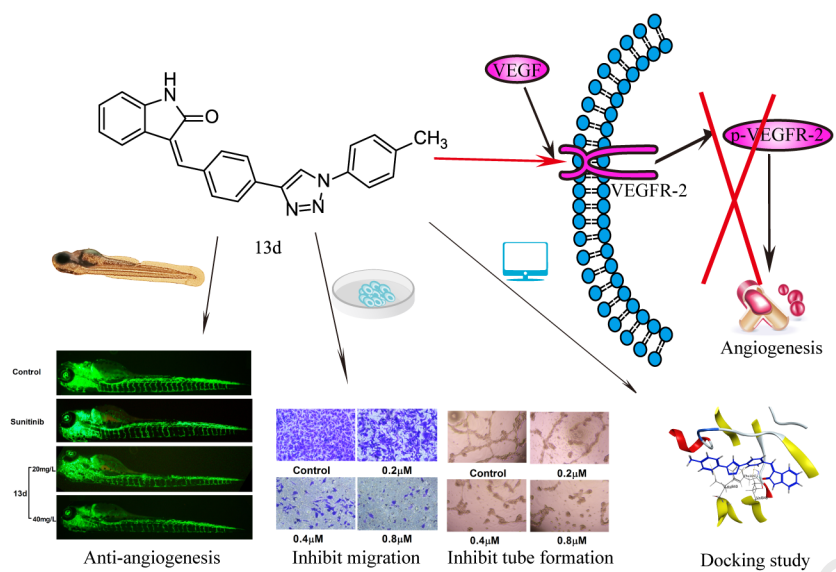
Accepted Date: 1 December 2020



Please cite this article as: D.-p. Wang, K.-l. Liu, X.-y. Li, G.-q. Lu, W.-h. Xue, X.-h. Qian, K. Mohamed O, F.-h. Meng, Design, synthesis, and *in vitro* and *in vivo* anti-angiogenesis study of a novel vascular endothelial growth factor receptor-2 (VEGFR-2) inhibitor based on 1,2,3-triazole scaffold, *European Journal of Medicinal Chemistry*, <https://doi.org/10.1016/j.ejmech.2020.113083>.

This is a PDF file of an article that has undergone enhancements after acceptance, such as the addition of a cover page and metadata, and formatting for readability, but it is not yet the definitive version of record. This version will undergo additional copyediting, typesetting and review before it is published in its final form, but we are providing this version to give early visibility of the article. Please note that, during the production process, errors may be discovered which could affect the content, and all legal disclaimers that apply to the journal pertain.

© 2020 Published by Elsevier Masson SAS.



**Design, synthesis, and *in vitro* and *in vivo* anti-angiogenesis study of a novel vascular endothelial growth factor receptor-2 (VEGFR-2) inhibitor based on 1,2,3-triazole scaffold**

De-pu Wang<sup>a,1</sup>, Kai-li Liu<sup>a,1</sup>, Xin-yang Li<sup>a,b</sup>, Guo-qing Lu<sup>a</sup>, Wen-han Xue<sup>a</sup>, Xin-hua Qian<sup>a</sup>, Kamara Mohamed O<sup>a</sup>, Fan-hao Meng<sup>a,\*</sup>

<sup>a</sup> School of Pharmacy, China Medical University, Shenyang, 110122, China.

<sup>b</sup> Department of Pharmacy, Shengjing Hospital of China Medical University, Shenyang, 110004, China.

\* Correspondence: Professor Fan-hao Meng, School of pharmacy, China Medical University, Shenyang, 77 Puhe Road, 110122, P. R. China.

E-mail: [fhmeng@cmu.edu.cn](mailto:fhmeng@cmu.edu.cn) Fax: +86-24-31939448

<sup>1</sup> The contributions of these authors are equal to this work.

1

2

3 **Abstract**

4 In the past five years, our team had been committed to click chemistry  
5 research, exploring the biological activity of 1,2,3-triazole by  
6 synthesizing different target inhibitors. In this study, a series of novel  
7 indole-2-one derivatives based on 1,2,3-triazole scaffolds were  
8 synthesized for the first time, and their inhibitory activity on vascular  
9 endothelial growth factor receptor-2 (VEGFR-2) was tested. Most of the  
10 compounds had shown promising activity in the VEGFR-2 kinase assay  
11 and had low toxicity to human umbilical vein endothelial cells  
12 (HUVECs). The compound **13d** ( $IC_{50} = 26.38$  nM) had better kinase  
13 activity inhibition ability than sunitinib ( $IC_{50} = 83.20$  nM) and was less  
14 toxic to HUVECs. Moreover, it had an excellent inhibitory effect on  
15 HT-29 and MKN-45 cells. On the one hand, by tube formation assay,  
16 transwell, and western blot analysis, compound **13d** could inhibit  
17 VEGFR-2 protein phosphorylate on HUVECs, thereby inhibiting  
18 HUVECs migration and tube formation. *In vivo* study, the zebrafish  
19 model with VEGFR-2 labeling also verified that compound **13d** had more  
20 anti-angiogenesis ability than sunitinib. On the other hand, molecular  
21 docking and molecular dynamics (MD) simulation results showed that  
22 compound **13d** could stably bind to the active site of VEGFR-2. Based on

the above findings, compound **13d** could be considered an effective anti-angiogenesis drug and has more development value than sunitinib.

**Keywords:** 1,2,3-Triazole; Anti-angiogenesis; VEGFR-2; Zebrafish.

## **1. Introduction**

Angiogenesis is the formation of new blood vessels by sprouting or splitting from pre-existing blood vessels [1-4]. It plays a critical role in the pathogenesis of various disorders, most notably growth and metastasis of solid tumors [5]. The growth and metastasis of tumors require new blood vessels to transport nutrients and oxygen [6]. Vascular endothelial growth factor (VEGF) is a highly specific vascular endothelial growth factor that is overexpressed in most solid tumors [7]. Excessive VEGF in solid tumors promotes the angiogenesis of adjacent blood vessels, and the excessive production of blood vessels can cause the imbalance of the metabolic microenvironment and accelerate tumor invasion and metastasis [6,8,9]. Therefore, anti-angiogenesis is an essential form of inhibiting tumor growth and metastasis [10-12].

Vascular endothelial growth factor receptor-2 (VEGFR-2), as the vital receptor of VEGF, which activated by VEGF initiates downstream signal transduction, ultimately leads to angiogenesis, tumor proliferation, and migration [7,13]. Therefore, a long-held concept that inhibition of VEGFR-2 would cause efficient anti-angiogenesis and antitumor response [14,15]. At present, the small molecule VEGFR-2 inhibitors

1 have emerged as promising anti-angiogenesis agents against a wide  
2 variety of cancers, such as sorafenib, cabozantinib, and sunitinib, and  
3 applied in clinical cancer therapy (**Fig. 1**) [16-18]. However,  
4 chemotherapy drugs can cause specific adverse side effects and affect  
5 patients' health [19]. Therefore, it is necessary to find low toxicity  
6 VEGFR-2 inhibitors with a novel structure to treat cancer and enrich  
7 VEGFR-2 inhibitors [7].

8 In the course of identifying various chemical fragments that could  
9 serve as a scaffold for novel anti-angiogenesis agents, our programs  
10 began with the indolin-2-one derivative sunitinib, a potent multitargeted  
11 kinase inhibitor of VEGFR-2, PDGFR, and c-KIT kinases [20-22]. The  
12 privileged indolin-2-one scaffold (red dashed rectangle in **Fig. 1**) was  
13 regarded as the most promising pharmacophore binding to the active site  
14 of VEGFR-2 kinase [23,24]. Moreover, it should be pointed out that  
15 numerous indolin-2-one derivatives have been reported as potent  
16 antitumor agents [23,25-28]. Therefore, the indolin-2-one scaffold was  
17 selected as a nucleus to develop a new VEGFR-2 inhibitor. The  
18 combination principle of multiple pharmacophores for developing a  
19 single molecule usually may enhance biological activity and improve  
20 bioavailability [29]. In our previous work, inspired by various biological  
21 properties of 1,2,3-triazole (blue dashed rectangle in **Fig. 1**), which could  
22 bind with biomolecular targets to fulfill its envisaged role as potential

1 pharmacophore [30-32], two series of 1,2,3-triazole derivatives (**TS-13n**,  
2 **B-10n** in **Fig. 1**) had been independently reported as potent antitumor  
3 agents in our laboratory [33-35].

4 Based on the findings mentioned earlier, we have been inspired to  
5 design and synthesize a series of novel derivatives derived by insertion of  
6 a 1,4-diphenyl-1*H*-1,2,3-triazole moiety on the active nucleus of  
7 indolin-2-one through an ethylene bridge (**Fig. 1**). Herein, twenty-eight  
8 novel indolin-2-one derivatives bearing 1,2,3-triazole moiety and their  
9 VEGFR-2 kinase inhibitory activity were reported. These derivatives  
10 exhibited potent inhibition of VEGFR-2 tyrosine kinase activity and  
11 efficiently inhibited angiogenesis with less toxicity *in vitro* and *in vivo*,  
12 suggesting that these derivatives could be considered promising lead  
13 compounds for further development of novel anti-angiogenesis agents.

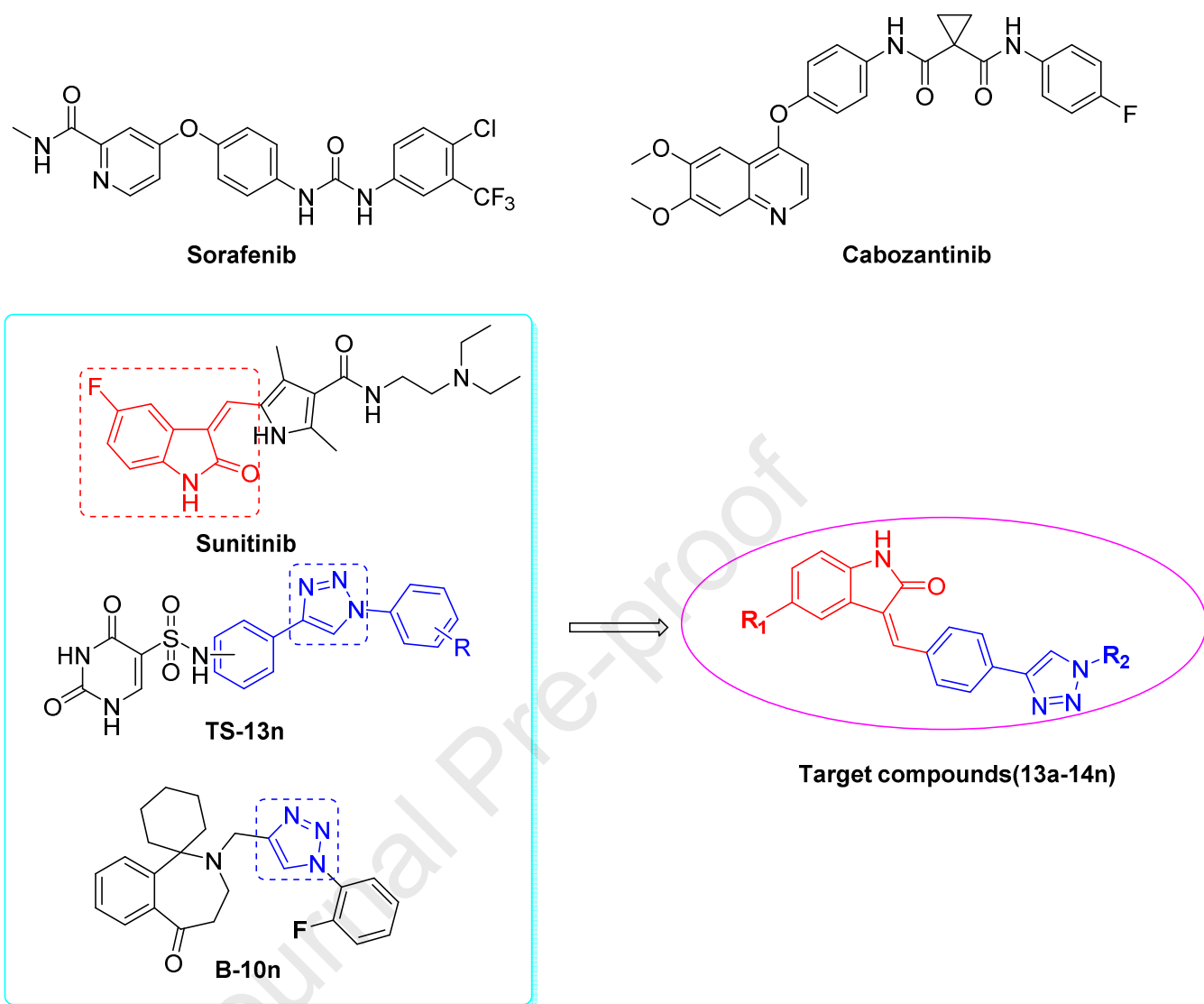


**Fig. 1.** Structures of sorafenib, cabozantinib, sunitinib, TS-13n, B-10n and design of the target compounds.

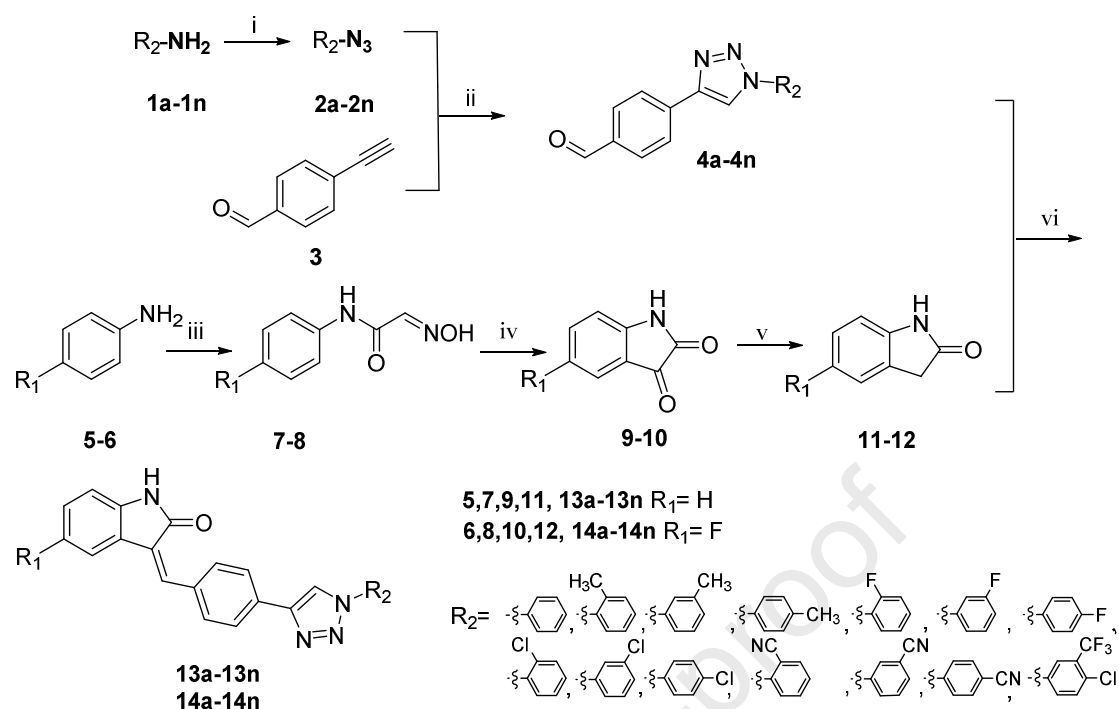
## 2. Results and discussion

### 2.1. Chemistry

The synthetic pathway adopted to prepare novel indole-2-one-1,2,3-triazole derivatives (**13a-14n**) was depicted in **Scheme 1**. First, the preparation of different substituted azide benzene (**2a-2n**) involved diazo-reaction and displacement reaction with sodium



1 azide ( $\text{NaN}_3$ ) (synthetic detail procedure is given in the Experimental  
2 section) [35]. Click chemistry is a practical approach for generating a  
3 1,2,3-triazole unit [34]. The novel intermediates (**4a-4n**) were obtained in  
4 high yields via Cu (I)-catalyzed azide-alkyne cycloaddition (CuAAC)  
5 between aryl-azides (**2a-2n**) and commercial 4-ethynylbenzaldehyde (**3**)  
6 in the presence of sodium ascorbate and  $\text{CuSO}_4 \cdot 5\text{H}_2\text{O}$  as a catalyst in  
7 DMF and water mixture as the solvent system [35]. The compounds **9-10**  
8 were prepared from compounds **5-6** via Sandmeyer's method described in  
9 the literature [37,38], reduced which using hydrazine hydrate to give  
10 compound **11-12** [39]. Finally, the title compounds (**13a-14n**) were  
11 accomplished by employing Claisen-Schmidt condensation reaction  
12 between indolin-2-ones (**11-12**) and various 1,2,3-triazole aromatic  
13 aldehydes (**4a-4n**) with a catalytic amount of piperidine as a base [40,  
14 41].



**Scheme 1.** Reagents and conditions: (i)  $NaNO_2$ ,  $HCl$ ,  $NaN_3$ ,  $CH_2Cl_2$ ,  $H_2O$ ,  $0-5^\circ C$ , 3-5 h; (ii)  $CuSO_4 \cdot 5H_2O$ , ascorbic acid,  $KI$ ,  $DMF$ ,  $H_2O$ ,  $50^\circ C$ , 6-10 h; (iii) chloral hydrate,  $Na_2SO_4$ ,  $NH_2OH \cdot HCl$ ,  $HCl$ ,  $H_2O$ ,  $85^\circ C$ , 3 h; (iv) conc  $H_2SO_4$ ,  $60^\circ C$ , 0.5 h,  $90^\circ C$  1.5 h; (v)  $N_2H_4 \cdot H_2O$ ,  $EtOH$ ,  $H_2O$ ,  $100^\circ C$ , 10 h; (vi)  $EtOH$ , piperidine,  $80^\circ C$ , 4-8 h.

The known intermediates **9-12** and novel intermediates **4a-4n** were characterized by melting points and spectroscopic techniques ( $^1H$  NMR, ESI-MS), and the target compounds (**13a-14n**) also were characterized by melting points and spectroscopic techniques ( $^1H$  NMR,  $^{13}C$  NMR, HRMS, and FT-IR). The melting points of intermediates **9-12** approximately matched with melting points data in existing literatures [42,43].

Since the indole-2-one derivative has an exocyclic double bond, the

1 target compounds could exist in the form of *E* or *Z* isomers. As for  
2 compound **13m**, **14a**, **14b**, **14j**, **14k**, and **14m**, the  $^1\text{H}$  NMR spectra  
3 revealed the existence of their inseparable *E/Z* mixtures, even the *E/Z*  
4 ratios using the corresponding chemical shifts and integrals. However,  
5 because we could not separate them from the silica gel column  
6 chromatography or conventional method, the  $^{13}\text{C}$  NMR spectra of these  
7 mixtures were not shown.

8 Although several documents had reported that the analogs of title  
9 compounds obtained in the similar synthetic method were  
10 *Z*-configurations [44,45], confirmation of the stereochemistry of  
11 indole-2-one-1,2,3-triazole derivatives still be requisite. Thus, the most  
12 potency compound **13d**, as the representative compound, was chosen to  
13 undergo the NOESY experiment. The NOE correlation (**Fig. 2**) between  
14  $\text{H}_6$  ( $\delta=7.73$  ppm) and  $\text{H}_{11}$  ( $\delta=7.85$  ppm) suggested that the isomer  
15 obtained correspond to *Z*-configuration (*Z*-**13d**), which should not exist in  
16 *E*-configuration (*E*-**13d**). This result also illustrated that other compounds  
17 (except **13m**, **14a**, **14b**, **14j**, **14k**, and **14m**) also were *Z* isomers.

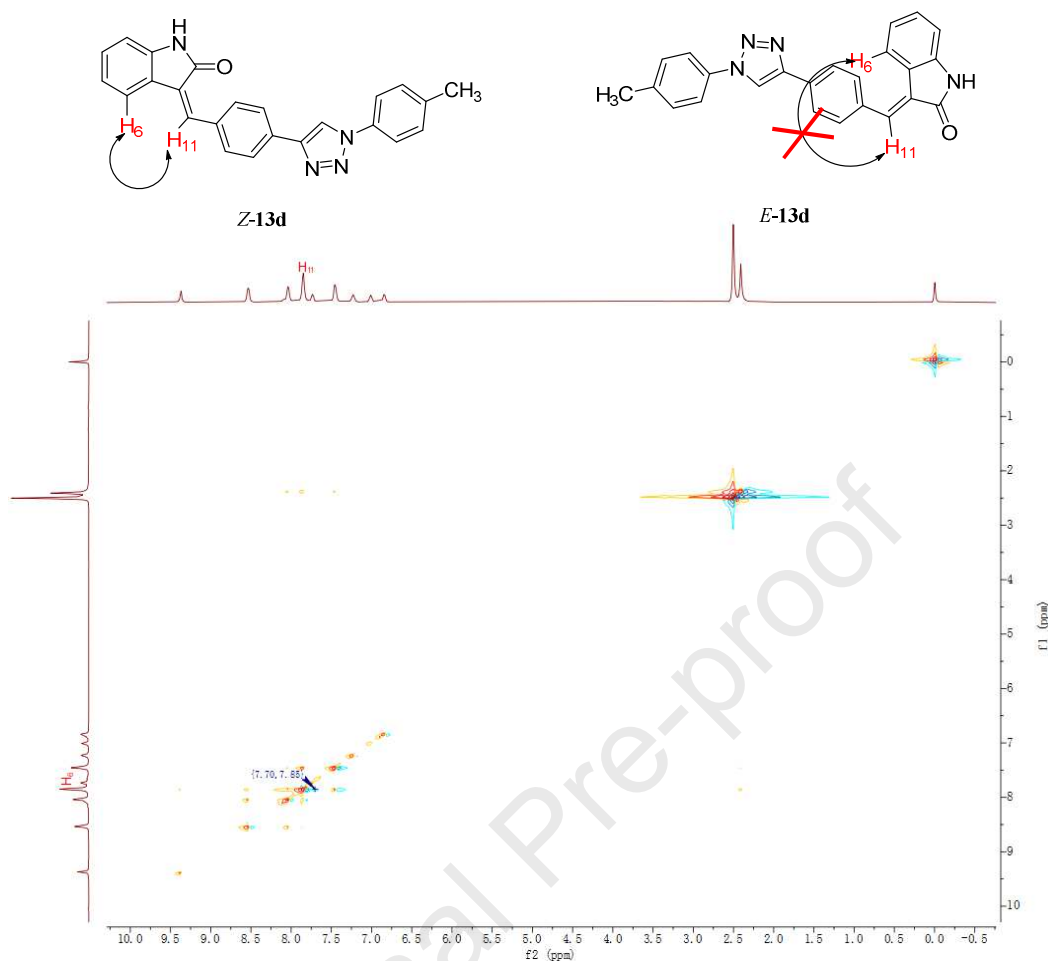


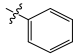
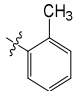
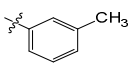
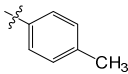
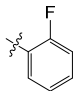
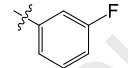
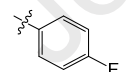
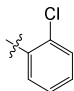
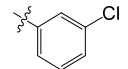
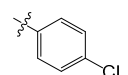
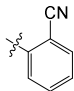
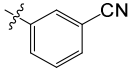
**Fig. 2.** NOESY of the representative compound **13d**.

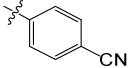
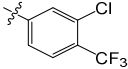
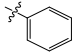
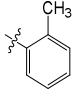
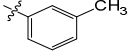
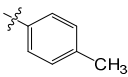
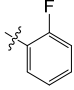
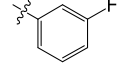
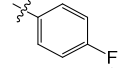
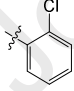
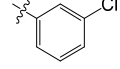
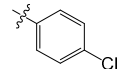
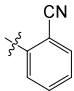
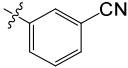
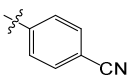
## 2.2. Biological evaluation

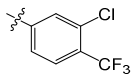
### 2.2.1. VEGFR-2 inhibitory assay in vitro and structure-activity relationship study (SAR)

To evaluate the inhibitory effects of sunitinib and all indole-2-one derivatives based on 1,2,3-triazole scaffolds (**13a-14n**) on VEGFR-2 kinase activity, VEGFR-2 inhibitory assay was carried out and the results were summarized in **Table 1**. Based on the VEGFR-2 kinase activity evaluation, the preliminary structure-activity relationship (SAR) in this work was summarized.

**Table 1.** The IC<sub>50</sub> value of compounds (**13a-14n**) and sunitinib against VEGFR-2, HT-29 cells, MKN-45 cells, and HUVECs.

Compd NO.	R <sup>1</sup>	R <sup>2</sup>	IC <sub>50</sub> <sup>a</sup>			
			VEGFR-2 (nM)	HT-29 (μM)	MKN-45(μM)	HUVECs (μM)
<b>13a</b>	H		93.11±1.95	7.07±1.10	11.59±0.81	12.68±1.69
<b>13b</b>	H		110.60±2.37	8.71±0.48	9.77±0.86	14.69±0.93
<b>13c</b>	H		44.67±0.94	3.94±0.38	4.69±0.24	13.70±0.13
<b>13d</b>	H		<b>26.38±1.09</b>	1.61±0.45	1.92±0.37	7.94±0.36
<b>13e</b>	H		115.42±2.37	10.53±0.79	12.54±0.97	19.26±1.07
<b>13f</b>	H		>200	>20	>20	>20
<b>13g</b>	H		198.54±1.37	17.73±3.80	16.70±0.82	14.71±0.23
<b>13h</b>	H		>200	>20	>20	>20
<b>13i</b>	H		>200	>20	>20	>20
<b>13j</b>	H		162.81±2.36	13.99±0.41	16.21±0.99	18.24±0.58
<b>13k</b>	H		169.42±1.45	14.39±1.44	14.63±0.53	19.72±1.02
<b>13l</b>	H		>200	>20	>20	>20

<b>13m</b>	H		178.91±1.36	15.78±2.55	>20	>20
<b>13n</b>	H		108.36±0.88	9.67±0.39	8.89±0.42	>20
<b>14a</b>	F		99.67±0.73	8.12±1.29	11.13±0.17	13.70±0.13
<b>14b</b>	F		71.55±0.16	5.87±0.32	7.21±1.90	8.63±0.27
<b>14c</b>	F		89.16±0.63	7.32±0.64	6.81±1.49	9.88±0.76
<b>14d</b>	F		36.90±0.54	3.98±0.61	34.62±0.34	13.83±0.42
<b>14e</b>	F		139.50±1.65	8.98±0.42	8.51±0.54	14.36±1.99
<b>14f</b>	F		171.12±1.09	12.97±0.72	8.19±1.30	17.25±1.22
<b>14g</b>	F		192.51±0.47	>20	>20	>20
<b>14h</b>	F		119.93±1.36	5.95±0.27	7.54±0.55	18.24±0.58
<b>14i</b>	F		186.44±1.02	10.46±0.43	14.08±0.88	19.42±0.59
<b>14j</b>	F		170.18±2.19	11.24±0.86	15.81±0.52	19.58±2.14
<b>14k</b>	F		187.24±2.88	13.98±0.43	15.21±0.73	>20
<b>14l</b>	F		193.41±0.97	>20	>20	>20
<b>14m</b>	F		190.07±1.98	>20	>20	>20

<b>14n</b>	F		168.89±2.34	16.52±0.77	>20	>20
<b>sunitinib</b>	-	-	83.20±1.36	10.34±0.96	9.25±0.77	6.37±0.59

1 a: IC<sub>50</sub> values are presented as mean values of at least three independent  
2 determinations.

3 We found that compared to the positive drug (sunitinib IC<sub>50</sub> = 83.20  
4 nM), most compounds exhibited excellent inhibitory activity against  
5 VEGFR-2. The semi-inhibitory concentration IC<sub>50</sub> value of seven  
6 compounds (**13a**, **13c**, **13d**, **14a-14d**) was less than 100 nM, which all  
7 showed excellent inhibition to VEGFR- 2. Furthermore, **13d** (IC<sub>50</sub> =  
8 26.38 nM) and **14d** (IC<sub>50</sub> = 36.9 nM) exhibited the best activities among  
9 them.

10 Moreover, we analyzed the effect of two substitutions of the  
11 indolin-2-one, **13a-13n** (R<sub>1</sub> = H) and **14a-14n** (R<sub>1</sub> = F) possessed similar  
12 IC<sub>50</sub> values for each comparison. It showed that the substitution effect of  
13 the indole-2-one part might not have too obvious value on the  
14 structure-activity relationship. Then, concerning the activity of  
15 derivatives with an unsubstituted or substituted phenyl group attached to  
16 triazole scaffold, incorporation of unsubstituted phenyl group or phenyl  
17 substituted by electron-donating groups led to compounds **13a-13d** and  
18 **14a-14d** with the better inhibitory action on VEGFR-2 relative to the  
19 electron-withdrawing groups substituted analogs (**13e-13n** and **14e-14n**).  
20 Furthermore, the activity of tolyl substituted and unsubstituted derivatives

1 was 4-CH<sub>3</sub>>3-CH<sub>3</sub>>2-CH<sub>3</sub>>H. Besides, there was no significant  
2 difference in the inhibitory activity between electron-withdrawing groups.

3 The results showed that the phenyl side groups substituted with  
4 electron-donor groups might significantly influence indole 1,2,3-triazole  
5 scaffolds' increased potency. In contrast, electron-withdrawing groups  
6 might have a common effect or decrease the inhibitory activities of  
7 scaffolds.

8 2.2.2. HT-29 cell lines, MKN-45 cell lines, HUVECs proliferation assay  
9 *in vitro*

10 CCK-8 assay was used to explore the effects of target compounds on  
11 the cell proliferation of human colon cancer (HT-29) cell lines, human  
12 gastric cancer (MKN-45) cell lines, and human umbilical vein endothelial  
13 cells (HUVECs). The positive control sunitinib was also conducted to  
14 assess the inhibitory abilities of cell proliferation of all compounds,  
15 shown as IC<sub>50</sub> values, and summarized in **Table 1**. Including the most  
16 potency compound **13d** verified by the VEGFR-2 kinase inhibition assay,  
17 the target compounds' overall toxicity to HUVECs was lower than that of  
18 sunitinib. Furthermore, compound **13d** had a good effect on inhibiting cell  
19 viability for HT-29 and MKN-45 cells. Interestingly, combined with the  
20 VEGFR-2 kinase inhibition assay results, the compound **13d** could inhibit  
21 the kinase activity of VEGFR-2 more effectively than sunitinib *in vitro*  
22 and simultaneously had less toxic to HUVECs.



### 2.2.3. Anti-angiogenesis effect *in vitro*

Based on the above experimental results, compound **13d** had the most potential to become a VEGFR-2 inhibitor. Therefore, the inhibitory effect of compound **13d** on angiogenesis was further explored. Transwell was used to explore the inhibitory ability of compound **13d** on HUVEC cell migration, and the results were shown in **Fig. 3A**. As the compound concentration increased, the migration ability of HUVECs decreased, signified that the changes have occurred in a concentration-dependent manner. Since compound **13d** was less toxic to HUVECs at low concentrations, the facts excluded the migratory inhibition of compound **13d** caused by toxic effects. At the same time, HUVECs were treated with the same concentration of compound **13d** to explore its effect on HUVECs' ability to form tubules, and the results were shown in **Fig. 3B**. Similarly, the tube formative length decreased with the concentration of **13d** increased.

These data indicated that compound **13d** could inhibit HUVECs migration and tube formation *in vitro*, which was an essential step in inhibiting angiogenesis.

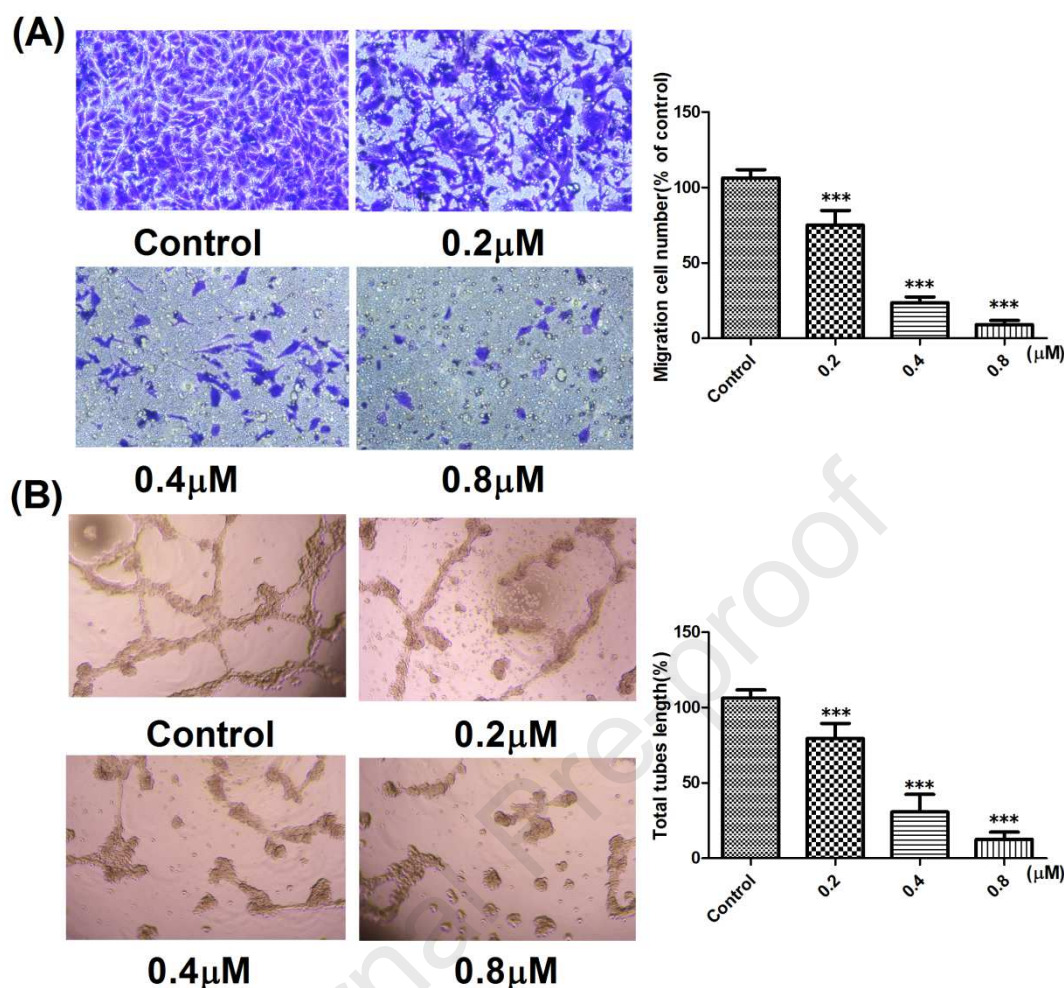


**Fig. 3.** Compound **13d** inhibited HUVECs migration and the tube formation. (A) Transwell analyzed the inhibitory effects of compound **13d** on HUVECs migration. (B) Effects of compound **13d** on the tube formation of HUVECs *in vitro*.

#### 2.2.4. Western blot analysis and anti-angiogenesis research *in vivo*.

Furthermore, Western blot was carried out to analyze VEGFR-2 protein's phosphorylation on HUVECs cell membranes at different compound concentrations. The results were shown in **Figure 4A**. As the concentration of compound **13d** increased, the phosphorylation of VEGFR-2 in HUVECs decreased. That is, the activation of VEGFR-2

1 decreased. Simultaneously, to verify the effect of compound **13d** on  
2 inhibiting angiogenesis *in vivo*, four groups of blood vessel-specific  
3 fluorescent transgenic zebrafish, in a total of 40, were used for  
4 anti-angiogenesis research. Zebrafish is currently the ideal vascular  
5 biology research and anti-tumor angiogenesis drug evaluation model,  
6 which can intuitively observe angiogenesis. The results were shown in  
7 **Fig. 4B**. At a 40 mg/L concentration, compound **13d** had a better  
8 inhibitory effect on zebrafish internode vascular (ISV) angiogenesis than  
9 sunitinib. Also, compound **13d** even effectively inhibited zebrafish ISV  
10 regeneration at a lower concentration (20 mg/L).

11 In general, compound **13d** could effectively inhibit the phosphorylation  
12 of VEGFR-2 with better anti-angiogenesis ability than sunitinib *in vivo*.  
13 These results were significantly different.

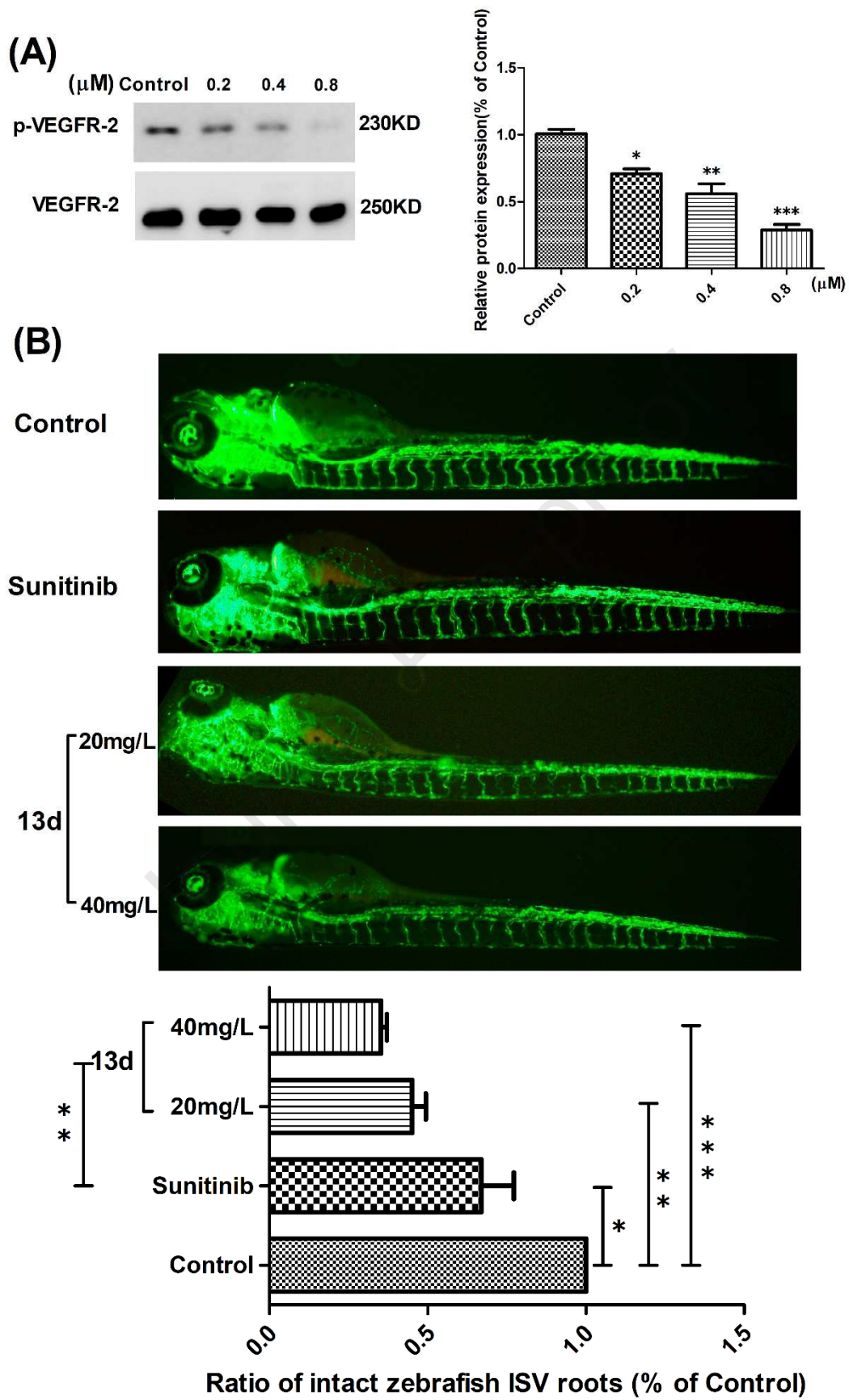


**Fig. 4.** The compound **13d** could inhibit the phosphorylation of VEGFR-2 and the angiogenesis of zebrafish microvessels. **(A)** Western blot analysis of the phosphorylation changes of VEGFR-2 with increasing compound **13d** concentration. **(B)** The effects of compound **13d** and sunitinib on the neovascularization of zebrafish *in vivo*.

### 2.3. Molecular modeling

#### 2.3.1. Molecular docking study

Molecular docking simulations were performed using MOE (Molecular Operating Environment, version 2016.08, Chemical Computing Group Inc., Canada) software to study the possible binding pattern of target compounds in the active site of VEGFR-2. Moreover, the crystal structure of VEGFR-2 in complex with sunitinib (PDB ID: 4AGD) was adopted in the docking calculations. The best docking conformation of the potent compound **13d** based on the compound activity against VEGFR-2 kinase was selected as the most probable binding conformation. The positive drug sunitinib, as the co-crystallized ligand, was re-docked using the same procedure as **13d**.

The re-docking result demonstrated that sunitinib (**Fig. 5B**) could stack well with the original ligand (**Fig. 5A**), two H-bonds predicted by the simulation of sunitinib were exactly the same to those existed in the crystal structure, and the Arene-H conjugates were roughly the same. These data strongly certified the feasibility of the simulation and

1 rationalized the predictive interactions of the compound **13d** with  
2 VEGFR-2 (**Fig. 5C**).

3 The docking conformation of compound **13d** in the binding site  
4 showed that carbonyl on the indole fragment formed a strong H-bond  
5 with Phe1047, the lateral phenyl and the phenyl group linked to the  
6 indole formed Arene-H conjugates with Val848 and Leu840, respectively.  
7 By contrast, either H-bonds or the Arene-H interactions of **13d** were less  
8 than sunitinib. Simultaneously, as a whole molecule, **13d** spatially  
9 extended more in-depth into the pocket of protein; this provided a  
10 reasonable explanation that compound **13d** had better kinase activity  
11 inhibition ability than sunitinib, which was confirmed by the VEGFR-2  
12 kinase assay.



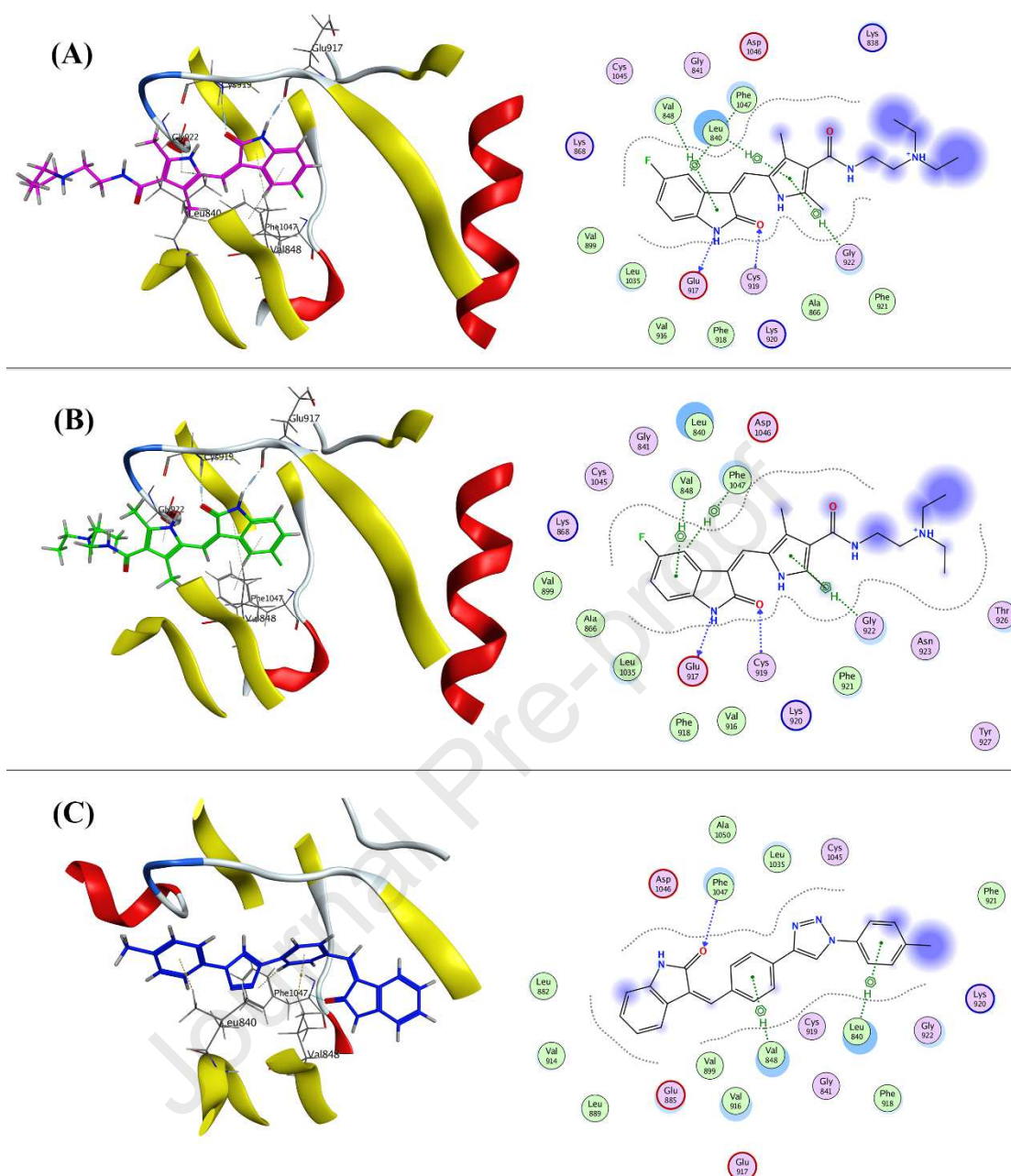


**Fig. 5.** The 2D diagram and 3D representation of original ligand (**A**), sunitinib (**B**) and compound **13d** (**C**) showing their interactions with the VEGFR-2 active site (PDB code: 4AGD).

### 2.3.2. Molecular dynamics (MD) simulation

Based on the compound activity against VEGFR-2 kinase, the docking conformation of the potent compound **13d** obtained in MOE (Molecular

Operating Environment) was selected to conduct molecular dynamics (MD) simulation in-depth the binding pose. MD simulation was then carried out in explicit aqueous solution for 10 ns. For comparison, MD simulation of positive control sunitinib in complex with VEGFR-2 was also performed.

The stability of two systems under simulation was evaluated by the root-mean-square deviation (RMSD) of the backbone atoms related to the starting structures (**Fig. 6**). As can be seen in the plots, all systems were stable during the 10-ns MD simulation; the values of RMSD of compound **13d** remained between 2 and 2.5 Å after reaching the summit, which demonstrated that the hit compound **13d** was stabilized in the active site.

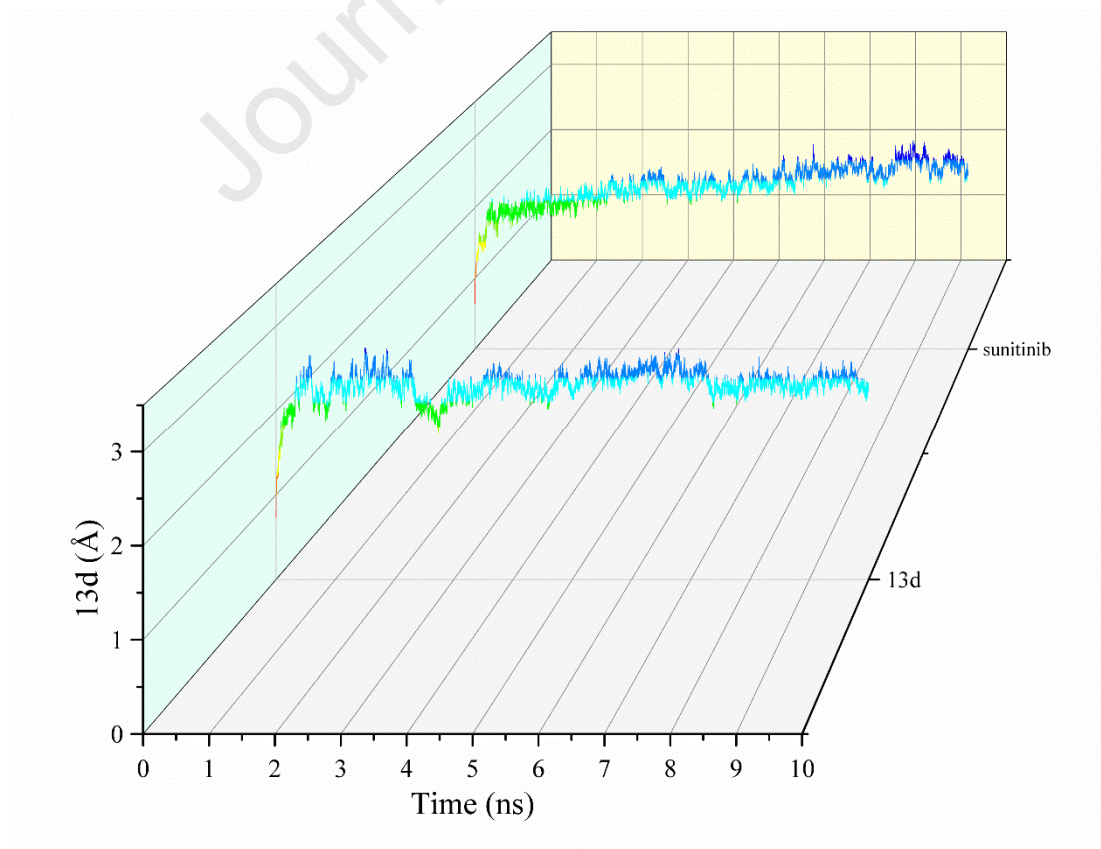




**Fig. 6.** RMSD tendency of two systems (**13d** and sunitinib) versus time in the 10 ns MD simulation.

#### 2.4. Toxicity prediction

**Table 2.** The pharmacokinetic studies of **13d** and sunitinib.

Compound NO.	Pharmacokinetic studies			
	Water solubility <sup>b</sup>	Plasma protein binding <sup>c</sup>	Acute Oral Toxicity <sup>d</sup>	Tetrahymena pyriformis <sup>e</sup>
<b>13d</b>	-3.051	0.831	1.773	1.299
<b>Sunitinib</b>	-3.217	0.914	2.683	1.653

<sup>b</sup> unit: logS; <sup>c</sup> unit: 100%; <sup>d</sup> unit: kg/mol; <sup>e</sup> unit: pIGC<sub>50</sub> (ug/L).

As a comprehensive and open-source tool, admetSAR was used to predict **13d** and sunitinib's toxicity, and the results were shown in **Table 2** [46]. Since the acute oral toxicity units and Tetrahymena pyriformis are kg/mol and pIGC<sub>50</sub> (ug/L), respectively (the lower value represents the lower toxicity), compound **13d** had low toxicity than sunitinib in both toxicity prediction assays, which inconsistent with the result of HUVECs proliferation assay.

### 3. Conclusion

The newly synthesized indolin-2-one derivatives based on 1,2,3-triazole scaffolds, evaluated as VEGFR-2 inhibitors, showed promising activity in the VEGFR-2 kinase inhibition assay. Among them, compound **13d** showed better activity inhibition on VEGFR-2 and lowered toxicity to HUVECs, and had an excellent inhibitory effect on HT-29 and MKN-45 cells than sunitinib. Transwell and tube formation experiments showed that compound **13d** inhibited HUVECs migration

1 and tube formation ability in a concentration-dependent manner.  
2 Furthermore, western blot analysis manifested compound **13d** could  
3 decrease the phosphorylation of VEGFR-2 in HUVECs. At the same time,  
4 by using VEGFR-2 specific fluorescent transgenic zebrafish, the  
5 inhibitory effect of compound **13d** on angiogenesis was verified *in vivo*.  
6 Besides, the rationality and scientificity of molecular design were verified  
7 by docking research and molecular dynamics simulation.

8 In conclusion, we designed and synthesized compound **13d** as a novel  
9 VEGFR-2 inhibitor that is more effective, less toxic than sunitinib.  
10 Compound **13d** provided a better choice for drug research and the  
11 development of new VEGFR-2 inhibitors.

## 12 **4. Experimental**

### 13 *4.1. Chemistry*

#### 14 *4.1.1. General methods*

15 Unless otherwise stated, all chemical reagents and solvents were  
16 purchased from commercial sources and can be used without further  
17 purification. Melting points were measured on a capillary electrothermal  
18 melting point apparatus without calibration. By thin layer  
19 chromatography (TLC), using GF254 silica gel from Qingdao Ocean  
20 Chemical Company (Qingdao, China), the reaction progress was  
21 monitored with a fluorescent indicator on a 254nm glass plate and  
22 visualized by ultraviolet light. Column chromatography was performed

1 using silica gel (200-300 mesh) from Qingdao Ocean Chemical Company  
2 (Qingdao, China), recorded  $^1\text{H}$  NMR and  $^{13}\text{C}$  NMR spectra on a Bruker  
3 AMX500 ( $^1\text{H}$  at 500 MHz,  $^{13}\text{C}$  at 126 MHz) magnetic resonance  
4 spectrometer at ambient temperature. All NMR spectra were recorded  
5 using  $\text{DMSO}-d_6$  as a solvent, and chemical shifts were reported in ppm  
6 (parts per million) relative to tetramethylsilane (TMS) as an internal  
7 standard.

#### 8 *4.1.2. The synthesis of substituted azido benzenes (2a-2n)*

9 Compound **2a** was synthesized by using the following procedure: To a  
10 stirred solution of aniline (**1a**) (3.00 g, 32.21 mmol) in dichloromethane  
11 (120 mL) were added 30 mL of aqueous  $\text{NaNO}_2$  (2.67 g, 38.66 mmol)  
12 solution and 37% concentrated hydrochloric acid (HCl) (3 mL)  
13 successively. After 0.5 h of stirring at  $0^\circ\text{C}$ , a solution of sodium azide  
14 ( $\text{NaN}_3$ ) (2.93 g, 45.10 mmol) dissolved in water (20 mL) was added  
15 dropwise, and the reaction mixture was kept stirring at  $0-5^\circ\text{C}$  for 3-5 h.  
16 The progress of the reaction was monitored through the TLC test. After  
17 the reaction was completed, the organic phase was separated and washed  
18 with brine, dried over anhydrous  $\text{Na}_2\text{SO}_4$ , filtered, and the solvent was  
19 removed under reduced pressure. The residue was purified by column  
20 chromatography on silica gel using petroleum ether to afford the title  
21 compound as pale yellow oil liquid.

22 Compounds **2b-2n** were prepared using the identical synthetic

1 procedure as **2a**.

2 *4.1.3. The synthesis of substituted azido benzenes (4a-4n)*

3 Compound **4a** was synthesized by using the following procedure:

4 Reaction of commercially 4-ethynylbenzaldehyde (**3**) (1.00 g, 7.68 mmol)  
5 with azidobenzene (**2a**) (1.01 g, 8.45 mmol) in 15 mL of DMF proceeded  
6 at 50°C for 5 h in the presence of 4 mL of aqueous copper sulfate  
7 pentahydrate ( $\text{CuSO}_4 \cdot 5\text{H}_2\text{O}$ ) (0.15 g, 0.60 mmol), ascorbic acid (0.15 g,  
8 0.85 mmol) and a catalytic amount of KI. The progress of the reaction  
9 was monitored through the TLC test. After the reaction was completed,  
10 the reaction was added 100 mL of water and extracted with ethyl acetate  
11 (3×100 mL). The combined extracts were washed with brine, dried over  
12 anhydrous  $\text{Na}_2\text{SO}_4$ , filtered, and the solvent was removed under reduced  
13 pressure. The crude residue was purified by column chromatography on  
14 silica gel using ethyl acetate/petroleum ether to afford the title compound  
15 as pale yellow solid.

16 Compounds **4b-4n** were prepared using the identical synthetic  
17 procedure as **4a**.

18 *4.1.3.1. 4-(1-phenyl-1H-1,2,3-triazol-4-yl)benzaldehyde (4a)*

19 Light yellow solid, yield: 49.52%, mp: 187.3°C.  $^1\text{H}$  NMR (500 MHz,  
20  $\text{DMSO}-d_6$ )  $\delta$  10.04 (s, 1H, CHO), 9.50 (s, 1H, H-triazole), 8.18 (d,  $J = 7.6$   
21 Hz, 2H, Ar-H), 8.05 (d,  $J = 7.5$  Hz, 2H, Ar-H), 7.97 (d,  $J = 7.8$  Hz, 2H,  
22 Ar-H), 7.65 (t,  $J = 7.4$  Hz, 2H, Ar-H), 7.54 (t,  $J = 7.3$  Hz, 1H, Ar-H).

1 ESI-MS  $[M+H]^+$  m/z: 250.13.

2 *4.1.3.2. 4-[1-(o-tolyl)-1H-1,2,3-triazol-4-yl]benzaldehyde (4b)*

3 Light yellow solid, yield: 45.15%, mp: 119.4°C.  $^1\text{H}$  NMR (500 MHz,  
4 DMSO- $d_6$ )  $\delta$  10.04 (s, 1H, CHO), 9.16 (d,  $J$  = 1.5 Hz, 1H, H-triazole),  
5 8.18 (s, 2H, Ar-H), 8.04 (d,  $J$  = 3.1 Hz, 2H, Ar-H), 7.52 (s, 3H, Ar-H),  
6 7.46 (s, 1H, Ar-H), 2.23 (s, 3H, CH<sub>3</sub>). ESI-MS  $[M+H]^+$  m/z: 264.15.

7 *4.1.3.3. 4-[1-(m-tolyl)-1H-1,2,3-triazol-4-yl]benzaldehyde (4c)*

8 Light brown solid, yield: 44.12%, mp: 174.4°C.  $^1\text{H}$  NMR (500 MHz,  
9 DMSO- $d_6$ )  $\delta$  10.04 (s, 1H, CHO), 9.48 (s, 1H, H-triazole), 8.17 (d,  $J$  = 7.7  
10 Hz, 2H, Ar-H), 8.04 (d,  $J$  = 7.7 Hz, 2H, Ar-H), 7.80 (s, 1H, Ar-H), 7.75 (d,  
11  $J$  = 7.5 Hz, 1H, Ar-H), 7.52 (t,  $J$  = 7.7 Hz, 1H, Ar-H), 7.35 (d,  $J$  = 7.0 Hz,  
12 1H, Ar-H), 2.44 (s, 3H, CH<sub>3</sub>). ESI-MS  $[M+H]^+$  m/z: 264.15.

13 *4.1.3.4. 4-[1-(p-tolyl)-1H-1,2,3-triazol-4-yl]benzaldehyde (4d)*

14 Light brown solid, yield: 46.14%, mp: 189.4-193.3°C.  $^1\text{H}$  NMR (500  
15 MHz, DMSO- $d_6$ )  $\delta$  10.04 (s, 1H, CHO), 9.46 (d,  $J$  = 1.8 Hz, 1H,  
16 H-triazole), 8.17 (d,  $J$  = 6.4 Hz, 2H, Ar-H), 8.04 (d,  $J$  = 6.4 Hz, 2H, Ar-H),  
17 7.84 (d,  $J$  = 6.4 Hz, 2H, Ar-H), 7.45 (d,  $J$  = 6.6 Hz, 2H, Ar-H), 2.40 (s, 3H,  
18 CH<sub>3</sub>). ESI-MS  $[M+H]^+$  m/z: 264.16.

19 *4.1.3.5. 4-[1-(2-fluorophenyl)-1H-1,2,3-triazol-4-yl]benzaldehyde (4e)*

20 Light yellow solid, yield: 46.26%, mp: 126.8°C.  $^1\text{H}$  NMR (500 MHz,  
21 DMSO- $d_6$ )  $\delta$  10.05 (s, 1H, CHO), 9.30 (s, 1H, H-triazole), 8.20 (d,  $J$  = 7.1  
22 Hz, 2H, Ar-H), 8.04 (d,  $J$  = 7.2 Hz, 2H, Ar-H), 7.93 (t,  $J$  = 7.6 Hz, 1H,

1 Ar-H), 7.64 (d,  $J = 10.4$  Hz, 2H, Ar-H), 7.49 (t,  $J = 6.8$  Hz, 1H, Ar-H).

2 ESI-MS  $[M+H]^+$  m/z: 268.10.

3 *4.1.3.6. 4-[1-(3-fluorophenyl)-1H-1,2,3-triazol-4-yl]benzaldehyde (4f)*

4 Light brown solid, yield: 44.25%, mp: 179.9°C.  $^1\text{H}$  NMR (500 MHz,  
5 DMSO- $d_6$ )  $\delta$  10.03 (s, 1H, CHO), 9.53 (s, 1H, H-triazole), 8.15 (d,  $J = 7.8$   
6 Hz, 2H, Ar-H), 8.04 (d,  $J = 7.8$  Hz, 2H, Ar-H), 7.90 – 7.83 (m, 2H, Ar-H),  
7 7.72 – 7.66 (m, 1H, Ar-H), 7.39 (t,  $J = 8.4$  Hz, 1H, Ar-H). ESI-MS  
8  $[M+H]^+$  m/z: 268.09.

9 *4.1.3.7. 4-[1-(4-fluorophenyl)-1H-1,2,3-triazol-4-yl]benzaldehyde (4g)*

10 Yellow solid, yield: 46.54%, mp: 203.5°C.  $^1\text{H}$  NMR (500 MHz,  
11 DMSO- $d_6$ )  $\delta$  10.04 (s, 1H, CHO), 9.47 (s, 1H, H-triazole), 8.16 (d,  $J = 6.8$   
12 Hz, 2H, Ar-H), 8.07 – 7.94 (m, 4H, Ar-H), 7.51 (dd,  $J = 9.1, 4.8$  Hz, 2H,  
13 Ar-H). ESI-MS  $[M+H]^+$  m/z: 268.10.

14 *4.1.3.8. 4-[1-(2-chlorophenyl)-1H-1,2,3-triazol-4-yl]benzaldehyde (4h)*

15 Light yellow solid, yield: 42.05%, mp: 121.3°C.  $^1\text{H}$  NMR (500 MHz,  
16 DMSO- $d_6$ )  $\delta$  10.04 (s, 1H, CHO), 9.26 (s, 1H, H-triazole), 8.19 (d,  $J = 7.8$   
17 Hz, 2H, Ar-H), 8.04 (d,  $J = 7.8$  Hz, 2H, Ar-H), 7.82 (t,  $J = 8.0$  Hz, 2H,  
18 Ar-H), 7.68 (t,  $J = 7.6$  Hz, 1H, Ar-H), 7.63 (t,  $J = 7.5$  Hz, 1H, Ar-H).  
19 ESI-MS  $[M+H]^+$  m/z: 284.03.

20 *4.1.3.9. 4-[1-(3-chlorophenyl)-1H-1,2,3-triazol-4-yl]benzaldehyde (4i)*

21 Light yellow solid, yield: 46.15%, mp: 191.4°C.  $^1\text{H}$  NMR (500 MHz,  
22 DMSO- $d_6$ )  $\delta$  10.04 (s, 1H, CHO), 9.57 (s, 1H, H-triazole), 8.15 (d,  $J = 6.1$

Hz, 2H, Ar-H), 8.09 (s, 1H, Ar-H), 8.04 (d,  $J = 4.7$  Hz, 2H, Ar-H), 7.98 (d,  $J = 6.3$  Hz, 1H, Ar-H), 7.68 (t,  $J = 6.2$  Hz, 1H, Ar-H), 7.61 (d,  $J = 6.1$  Hz, 1H, Ar-H). ESI-MS  $[M+H]^+$   $m/z$ : 284.13.

4.1.3.10. 4-[1-(4-chlorophenyl)-1H-1,2,3-triazol-4-yl]benzaldehyde (**4j**)

Light brown solid, yield: 38.95%, mp: 202.5°C.  $^1\text{H}$  NMR (500 MHz, DMSO- $d_6$ )  $\delta$  10.04 (s, 1H, CHO), 9.53 (s, 1H, H-triazole), 8.16 (d,  $J = 8.1$  Hz, 2H, Ar-H), 8.04 (d,  $J = 8.2$  Hz, 2H, Ar-H), 8.00 (d,  $J = 8.8$  Hz, 2H, Ar-H), 7.73 (d,  $J = 8.8$  Hz, 2H, Ar-H). ESI-MS  $[M+H]^+$   $m/z$ : 284.11.

4.1.3.11. 2-[4-(4-formylphenyl)-1H-1,2,3-triazol-1-yl]benzonitrile (**4k**)

Light brown solid, yield: 49.42%, mp: 217.5°C.  $^1\text{H}$  NMR (500 MHz, DMSO- $d_6$ )  $\delta$  10.06 (s, 1H, CHO), 9.44 (s, 1H, H-triazole), 8.20 (d,  $J = 7.7$  Hz, 3H, Ar-H), 8.07 (d,  $J = 7.8$  Hz, 2H, Ar-H), 8.01 (dt,  $J = 16.1, 7.9$  Hz, 2H, Ar-H), 7.82 (t,  $J = 7.5$  Hz, 1H, Ar-H). ESI-MS  $[M+H]^+$   $m/z$ : 275.12.

4.1.3.12. 3-[4-(4-formylphenyl)-1H-1,2,3-triazol-1-yl]benzonitrile (**4l**)

Light brown solid; yield: 43.19%, mp: 102.3°C.  $^1\text{H}$  NMR (500 MHz, DMSO- $d_6$ )  $\delta$  10.04 (s, 1H, CHO), 9.60 (s, 1H, H-triazole), 8.48 (s, 1H, Ar-H), 8.34 (d,  $J = 7.4$  Hz, 1H, Ar-H), 8.14 (d,  $J = 7.4$  Hz, 2H, Ar-H), 8.03 (dd,  $J = 21.2, 6.6$  Hz, 3H, Ar-H), 7.86 (t,  $J = 7.8$  Hz, 1H, Ar-H). ESI-MS  $[M+H]^+$   $m/z$ : 275.13.

4.1.3.13. 4-[4-(4-formylphenyl)-1H-1,2,3-triazol-1-yl]benzonitrile (**4m**)

Light brown solid, yield: 44.05%, mp: 113.5°C.  $^1\text{H}$  NMR (500 MHz, DMSO- $d_6$ )  $\delta$  10.04 (s, 1H, CHO), 9.64 (s, 1H, H-triazole), 8.19 (d,  $J = 8.8$

1 Hz, 2H, Ar-H), 8.15 (d,  $J = 6.7$  Hz, 4H, Ar-H), 8.04 (d,  $J = 8.1$  Hz, 2H,  
2 Ar-H). ESI-MS  $[M+H]^+$   $m/z$ : 275.10.

3 *4.1.3.14.*

4 *4-{1-[4-chloro-3-(trifluoromethyl)phenyl]-1H-1,2,3-triazol-4-yl}benzalde*  
5 *hyde (4n)*

6 Light yellow solid, yield: 45.64%, mp: 209.4 °C.  $^1\text{H}$  NMR (500 MHz,  
7 DMSO- $d_6$ )  $\delta$  10.03 (s, 1H, CHO), 9.66 (s, 1H, H-triazole), 8.40 (s, 1H,  
8 Ar-H), 8.30 (d,  $J = 8.7$  Hz, 1H, Ar-H), 8.13 (d,  $J = 7.9$  Hz, 2H, Ar-H),  
9 8.03 (t,  $J = 8.6$  Hz, 3H, Ar-H). ESI-MS  $[M+H]^+$   $m/z$ : 352.10.

10 *4.1.4. The synthesis of substituted 2-(hydroxyimino)- N- phenylacetamide*  
11 *(7-8)*

12 Compound **7** was synthesized by using the following procedure: To a  
13 stirred solution of anhydrous sodium sulfate (40.00 g, 281.62 mmol) in  
14 water (150 mL), chloral hydrate (10.00 g, 60.46 mmol) was added. Then  
15 the commercially aniline (**5**) (3.00 g, 32.21 mmol), 37% concentrated  
16 hydrochloric acid (3.6 mL), and hydroxylamine hydrochloride (8.30 g,  
17 119.45 mmol) were sequentially added. The mixture was stirred at 80 °C  
18 for 3 h. After the reaction was completed, the reaction system was cooled  
19 to room temperature, filtered and dried to obtain a crude product as a  
20 brown solid, which was used in the next step without purification.

21 Compound **8** were prepared using the identical synthetic procedure as  
22 **7**.



#### 4.1.5. The synthesis of substituted indoline-2,3-dione (**9-10**)

Compound **9** was synthesized by using the following procedure: A round bottom flask was charged with compound **7** (2.00 g, 12.18 mmol) and concentrated sulfuric acid H<sub>2</sub>SO<sub>4</sub> (30 mL). After 0.5 h of stirring at 60°C, the temperature of the reaction mixture was raised to 90°C for 1.5 h. After the reaction was completed, the reaction system was cooled to room temperature and poured into ice water (80 mL). The solid precipitate was filtered with suction, washed with water (4×50 mL) and dried. The crude residue was purified by column chromatography on silica gel using ethyl acetate/petroleum ether to obtain an orange solid (mp: 194°C).

Compound **10** (mp: 225°C) were prepared using the identical synthetic procedure as **9**.

#### 4.1.6. The synthesis of substituted indolin-2-one (**11-12**)

Compound **11** was synthesized by using the following procedure: To a solution of compound **9** (2.00 g, 14.00 mmol) in ethanol (50 mL) was added 80% hydrazine hydrate (12.78 g, 203.90 mmol) and water (30 mL). The reaction mixture was stirred at 100°C for 10 h. The progress of the reaction was monitored through the TLC test. After the reaction was completed, the solvent was removed under reduced pressure. The crude residue was purified by column chromatography on silica gel using ethyl acetate/petroleum ether to afford the title compound as pale yellow solid.

Compound **12** were prepared using the identical synthetic procedure as

**11.****4.1.6.1. indolin-2-one (11)**

Light yellow solid, yield: 72.06%, mp: 122.4°C. <sup>1</sup>H NMR (500 MHz, DMSO-*d*<sub>6</sub>) δ 10.38 (s, 1H, N-H), 7.22 – 7.11 (m, 2H, Ar-H), 6.91 (t, *J* = 7.4 Hz, 1H, Ar-H), 6.81 (d, *J* = 7.7 Hz, 1H, Ar-H), 3.45 (s, 2H, CH<sub>2</sub>). ESI-MS [M+H]<sup>+</sup> *m/z*: 134.03.

**4.1.6.2. 5-fluoroindolin-2-one (12)**

Light yellow solid, yield: 62.14%, mp: 142.4°C. <sup>1</sup>H NMR (500 MHz, DMSO-*d*<sub>6</sub>) δ 10.35 (s, 1H, N-H), 7.08 (d, *J* = 8.4 Hz, 1H, Ar-H), 6.97 (t, *J* = 9.4 Hz, 1H, Ar-H), 6.77 (d, *J* = 4.1 Hz, 1H, Ar-H), 3.48 (s, 2H, CH<sub>2</sub>). ESI-MS [M+H]<sup>+</sup> *m/z*: 152.06.

**4.1.7. The synthesis of target compounds (13a-14n)**

Compound **13a** was synthesized by using the following procedure: Reaction of indolin-2-ones (**11**) (1.00 g, 7.51mmol) with compound **4a** (2.06g, 8.26 mmol) in ethanol (35 mL) was proceeded at 80°C for 4-8 h in the presence of catalytic amount of piperidine. The progress of the reaction was monitored through the TLC test. After the reaction was completed, the reaction system was cooled to room temperature. The precipitate thus formed were collected by filtration, washed with ethanol (2×15 mL), and dried to yield pure target compound **13a** in moderate yield.

Compound **13b-14n** were prepared in moderate to good yields using

the identical synthetic procedure as **13a**.

#### 4.1.7.1.

*(Z)*-3-[4-(1-phenyl-1H-1,2,3-triazol-4-yl)benzylidene]indolin-2-one (**13a**)

Yellow powder, yield: 62.44%, mp: 243°C. FI-IR (KBr,  $\nu_{\max}$  cm<sup>-1</sup>): 3431 (NH), 1704 (C=O). <sup>1</sup>H NMR (500 MHz, DMSO-*d*<sub>6</sub>)  $\delta$  10.64 (s, 1H, N-H), 9.43 (s, 1H, H-triazole), 8.10 (d, *J* = 7.8 Hz, 2H, Ar-H), 7.98 (d, *J* = 7.7 Hz, 2H, Ar-H), 7.86 (d, *J* = 7.7 Hz, 2H, H-vinyl, Ar-H), 7.68 – 7.62 (m, 4H, Ar-H), 7.54 (t, *J* = 7.2 Hz, 1H, Ar-H), 7.25 (t, *J* = 7.5 Hz, 1H, Ar-H), 6.88 (t, *J* = 7.8 Hz, 2H, Ar-H). <sup>13</sup>C NMR (126 MHz, DMSO-*d*<sub>6</sub>)  $\delta$  168.48 (C=O), 146.59 (C-triazole), 142.88, 136.45 (C-vinyl), 135.06, 134.09, 131.24 (C-triazole), 130.07, 130.03 (2C), 129.82 (2C), 128.67, 127.57, 125.37 (2C), 122.34, 121.03, 120.74, 120.13 (C-vinyl), 119.92 (2C), 110.02. ESI-HRMS calcd for C<sub>23</sub>H<sub>17</sub>N<sub>4</sub>O [M+H]<sup>+</sup> 365.1324, found: 365.1398.

#### 4.1.7.2.

*(Z)*-3-{4-[1-(*o*-tolyl)-1H-1,2,3-triazol-4-yl]benzylidene}indolin-2-one (**13b**)

Orange powder, yield: 53.42%, mp: 239°C. FI-IR (KBr,  $\nu_{\max}$  cm<sup>-1</sup>): 3441 (NH), 1711 (C=O). <sup>1</sup>H NMR (500 MHz, DMSO-*d*<sub>6</sub>)  $\delta$  10.65 (s, 1H, N-H), 9.08 (s, 1H, H-triazole), 8.11 (d, *J* = 7.8 Hz, 2H, Ar-H), 7.85 (d, *J* = 7.7 Hz, 2H, H-vinyl, Ar-H), 7.67 (s, 1H, Ar-H), 7.63 (d, *J* = 7.6 Hz, 1H, Ar-H), 7.56 – 7.50 (m, 3H, Ar-H), 7.46 (s, 1H, Ar-H), 7.24 (t, *J* = 7.6 Hz,

1 1H, Ar-H), 6.94 – 6.84 (m, 2H, Ar-H), 2.24 (s, 3H, CH<sub>3</sub>). <sup>13</sup>C NMR (126  
 2 MHz, DMSO-*d*<sub>6</sub>)  $\delta$  168.50 (C=O), 145.77 (C-triazole), 142.88, 136.07  
 3 (C-vinylic), 135.11, 133.97, 132.91 (C-triazole), 132.53, 131.29, 129.99  
 4 (2C), 129.78, 127.55, 126.90, 125.83, 125.35 (2C), 124.76, 123.52,  
 5 122.33, 121.01 (C-vinylic), 120.77, 110.01, 17.31 (CH<sub>3</sub>). ESI-HRMS  
 6 calcd for C<sub>24</sub>H<sub>19</sub>N<sub>4</sub>O [M+H]<sup>+</sup> 379.1481, found: 379.1560.

7 4.1.7.3.

8 (*Z*)-3-{4-[1-(*m*-tolyl)-1*H*-1,2,3-triazol-4-yl]benzylidene}indolin-2-one  
 9 (**13c**)

10 Brown powder, yield: 64.61%, mp: 240 °C. FI-IR (KBr,  $\nu_{\max}$  cm<sup>-1</sup>): 3405  
 11 (NH), 1700 (C=O). <sup>1</sup>H NMR (500 MHz, DMSO-*d*<sub>6</sub>)  $\delta$  10.64 (s, 1H, N-H),  
 12 9.39 (s, 1H, H-triazole), 8.09 (d, *J* = 7.2 Hz, 2H, Ar-H), 7.85 (d, *J* = 7.3  
 13 Hz, 2H, H-vinylic, Ar-H), 7.81 (s, 1H, Ar-H), 7.76 (d, *J* = 7.5 Hz, 1H,  
 14 Ar-H), 7.66 (s, 1H, Ar-H), 7.63 (d, *J* = 7.5 Hz, 1H, Ar-H), 7.51 (t, *J* = 7.4  
 15 Hz, 1H, Ar-H), 7.33 (d, *J* = 6.9 Hz, 1H, Ar-H), 7.24 (t, *J* = 7.2 Hz, 1H,  
 16 Ar-H), 6.88 (t, *J* = 8.3 Hz, 2H, Ar-H), 2.44 (s, 3H, CH<sub>3</sub>). <sup>13</sup>C NMR (126  
 17 MHz, DMSO-*d*<sub>6</sub>)  $\delta$  168.49 (C=O), 146.51 (C-triazole), 142.88, 139.55  
 18 (C-vinylic), 136.40, 135.06, 134.06, 131.28 (C-triazole), 130.04, 130.01  
 19 (2C), 129.58, 129.22, 127.56, 125.34 (2C), 122.33, 121.01, 120.75,  
 20 120.30, 120.04 (C-vinylic), 116.98, 110.01, 20.79 (CH<sub>3</sub>). ESI-HRMS  
 21 calcd for C<sub>24</sub>H<sub>19</sub>N<sub>4</sub>O [M+H]<sup>+</sup> 379.1481, found: 379.1550.

22 4.1.7.4.

1 (Z)-3-{4-[1-(p-tolyl)-1H-1,2,3-triazol-4-yl]benzylidene}indolin-2-one

2 (**13d**)

3 Yellow powder, yield: 51.64%, mp: 248°C. FI-IR (KBr,  $\nu_{\max}$  cm<sup>-1</sup>):

4 3427 (NH), 1692 (C=O). <sup>1</sup>H NMR (500 MHz, DMSO-*d*<sub>6</sub>)  $\delta$  10.63 (s, 1H,

5 N-H), 9.35 (s, 1H, H-triazole), 8.53 (d, *J* = 8.2 Hz, 2H, Ar-H), 8.03 (d, *J* =

6 8.2 Hz, 2H, Ar-H), 7.85 (d, *J* = 7.3 Hz, 3H, H-vinyllic, Ar-H), 7.73 (d, *J* =

7 7.4 Hz, 1H, Ar-H), 7.45 (d, *J* = 7.9 Hz, 2H, Ar-H), 7.23 (t, *J* = 7.6 Hz, 1H,

8 Ar-H), 7.01 (t, *J* = 7.5 Hz, 1H, Ar-H), 6.84 (d, *J* = 7.7 Hz, 1H, Ar-H), 2.41

9 (s, 3H, CH<sub>3</sub>). <sup>13</sup>C NMR (126 MHz, DMSO-*d*<sub>6</sub>)  $\delta$  166.99 (C=O), 146.58

10 (C-triazole), 140.67, 138.34 (C-vinyllic), 135.86, 134.23, 133.65, 132.50

11 (2C), 131.75 (C-triazole), 130.13 (2C), 128.85, 126.72, 125.37, 124.76

12 (2C), 120.93, 120.11 (C-vinyllic), 119.85 (2C), 119.65, 109.23, 20.44

13 (CH<sub>3</sub>). ESI-HRMS calcd for C<sub>24</sub>H<sub>19</sub>N<sub>4</sub>O [M+H]<sup>+</sup> 379.1481, found:

14 379.1550.

15 4.1.7.5. (Z)-3-{4-[1-(2-fluorophenyl)-1H-1,2,3-triazol-4-yl]benzylidene}

16 indolin-2-one (**13e**)

17 Yellow powder, yield: 57.81%, mp: 234°C. FI-IR (KBr,  $\nu_{\max}$  cm<sup>-1</sup>):

18 3504 (NH), 1693 (C=O). <sup>1</sup>H NMR (500 MHz, DMSO-*d*<sub>6</sub>)  $\delta$  10.63 (s, 1H,

19 N-H), 9.19 (s, 1H, H-triazole), 8.12 (d, *J* = 7.9 Hz, 2H, Ar-H), 7.93 (t, *J* =

20 7.8 Hz, 1H, Ar-H), 7.85 (d, *J* = 8.0 Hz, 2H, H-vinyllic, Ar-H), 7.68 – 7.59

21 (m, 4H, Ar-H), 7.48 (t, *J* = 7.6 Hz, 1H, Ar-H), 7.24 (t, *J* = 7.7 Hz, 1H,

22 Ar-H), 6.88 (dd, *J* = 13.5, 7.3 Hz, 2H, Ar-H). <sup>13</sup>C NMR (126 MHz,

1 DMSO- $d_6$ )  $\delta$  168.47 (C=O), 154.69, 152.70, 146.21 (C-triazole), 142.88,  
 2 135.02 (C-vinylic), 134.17, 132.50 (C-triazole), 130.99, 130.01 (d,  $J$  =  
 3 6.0 Hz, 2C, C-fluorobenzene), 127.60, 125.83 (d,  $J$  = 3.3 Hz,  
 4 C-fluorobenzene), 125.44 (d,  $J$  = 4.6 Hz, 2C, C-fluorobenzene), 124.86  
 5 (C-vinylic), 123.25 (d,  $J$  = 4.1 Hz, C-fluorobenzene), 122.33, 121.00,  
 6 120.74, 117.11, 116.96, 110.00. ESI-HRMS calcd for  $C_{23}H_{16}FN_4O$   
 7  $[M+H]^+$  383.1230, found: 383.1307.

8 4.1.7.6. (Z)-3-{4-[1-(3-fluorophenyl)-1H-1,2,3-triazol-4-yl]benzylidene}  
 9 indolin-2-one (**13f**)

10 Yellow powder, yield: 63.46%, mp: 246°C. FI-IR (KBr,  $\nu_{\max}$   $\text{cm}^{-1}$ ):  
 11 3286 (NH), 1687 (C=O).  $^1\text{H}$  NMR (500 MHz, DMSO- $d_6$ )  $\delta$  10.66 (s, 1H,  
 12 N-H), 9.45 (s, 1H, H-triazole), 8.53 (d,  $J$  = 8.0 Hz, 2H, Ar-H), 8.02 (d,  $J$  =  
 13 7.9 Hz, 2H, Ar-H), 7.90 – 7.81 (m, 3H, H-vinylic, Ar-H), 7.70 (dd,  $J$  =  
 14 19.4, 7.4 Hz, 2H, Ar-H), 7.38 (t,  $J$  = 8.3 Hz, 1H, Ar-H), 7.22 (t,  $J$  = 7.4 Hz,  
 15 1H, Ar-H), 7.00 (t,  $J$  = 7.4 Hz, 1H, Ar-H), 6.83 (d,  $J$  = 7.6 Hz, 1H, Ar-H).  
 16  $^{13}\text{C}$  NMR (126 MHz, DMSO- $d_6$ )  $\delta$  166.98 (C=O), 163.28, 161.33, 146.80  
 17 (C-triazole), 140.69, 135.78 (C-vinylic), 133.79 (C-triazole), 132.52 (2C),  
 18 131.75 (d,  $J$  = 9.4 Hz, C-fluorobenzene), 131.41, 130.05 (d,  $J$  = 4.1 Hz,  
 19 C-fluorobenzene), 128.87, 126.81, 125.39, 124.78 (2C), 120.92, 120.38  
 20 (C-vinylic), 119.66, 115.83 (d,  $J$  = 3.4 Hz, C-fluorobenzene), 109.23,  
 21 107.29 (d,  $J$  = 3.3 Hz, C-fluorobenzene). ESI-HRMS calcd for  
 22  $C_{23}H_{16}FN_4O$   $[M+H]^+$  383.1230, found: 383.1298.

1 4.1.7.7. (Z)-3-{4-[1-(4-fluorophenyl)-1H-1,2,3-triazol-4-yl]benzylidene}  
 2 indolin-2-one (**13g**)

3 Yellow powder, yield: 63.91%, mp: 238°C. FI-IR (KBr,  $\nu_{\max}$  cm<sup>-1</sup>):  
 4 3448 (NH), 1686 (C=O). <sup>1</sup>H NMR (500 MHz, DMSO-*d*<sub>6</sub>)  $\delta$  10.66 (s, 1H,  
 5 N-H), 9.35 (s, 1H, H-triazole), 8.52 (d, *J* = 7.7 Hz, 2H, Ar-H), 8.01 (d, *J* =  
 6 7.6 Hz, 4H, Ar-H), 7.81 (s, 1H, H-vinyl), 7.71 (d, *J* = 7.1 Hz, 1H, Ar-H),  
 7 7.49 (t, *J* = 8.1 Hz, 2H, Ar-H), 7.21 (t, *J* = 7.1 Hz, 1H, Ar-H), 6.99 (t, *J* =  
 8 7.1 Hz, 1H, Ar-H), 6.83 (d, *J* = 7.3 Hz, 1H, Ar-H). <sup>13</sup>C NMR (126 MHz,  
 9 DMSO-*d*<sub>6</sub>)  $\delta$  166.96 (C=O), 162.55, 160.60, 146.69 (C-triazole), 140.66,  
 10 135.82 (C-vinyl), 133.70 (C-triazole), 133.00 (d, *J* = 3.0 Hz,  
 11 C-fluorobenzene), 132.51 (2C), 131.58, 130.02, 128.86, 126.74, 125.35,  
 12 124.76 (d, *J* = 3.2 Hz, 2C, C-fluorobenzene), 122.32 (d, *J* = 8.9 Hz),  
 13 120.92 (C-vinyl), 120.51, 119.65, 116.65 (d, *J* = 23.3 Hz,  
 14 C-fluorobenzene), 109.21. ESI-HRMS calcd for C<sub>23</sub>H<sub>16</sub>FN<sub>4</sub>O [M+H]<sup>+</sup>  
 15 383.1230, found: 383.1313.

16 4.1.7.8. (Z)-3-{4-[1-(2-chlorophenyl)-1H-1,2,3-triazol-4-yl]benzylidene}  
 17 indolin-2-one (**13h**)

18 Yellow powder, yield: 64.14%, mp: 229°C. FI-IR (KBr,  $\nu_{\max}$  cm<sup>-1</sup>):  
 19 3431 (NH), 1710 (C=O). <sup>1</sup>H NMR (500 MHz, DMSO-*d*<sub>6</sub>)  $\delta$  10.63 (s, 1H,  
 20 N-H), 9.17 (s, 1H, H-triazole), 8.11 (d, *J* = 7.9 Hz, 2H, Ar-H), 7.89 – 7.78  
 21 (m, 4H, H-vinyl, Ar-H), 7.71 – 7.60 (m, 4H, Ar-H), 7.24 (t, *J* = 7.7 Hz,  
 22 1H, Ar-H), 6.88 (t, *J* = 9.0 Hz, 2H, Ar-H). <sup>13</sup>C NMR (126 MHz,

1 DMSO- $d_6$ )  $\delta$  168.47 (C=O), 145.81 (C-triazole), 142.89, 135.86  
 2 (C-vinyllic), 135.05, 134.32, 132.55, 131.70, 131.11 (C-triazole), 130.47,  
 3 130.02 (2C), 128.39, 128.29, 127.63, 125.41 (2C), 124.80, 124.08, 122.35,  
 4 121.03 (C-vinyllic), 119.66, 110.02. ESI-HRMS calcd for  $C_{23}H_{16}ClN_4O$   
 5  $[M+H]^+$  399.0934, found: 399.1011.

6 4.1.7.9. (Z)-3-{4-[1-(3-chlorophenyl)-1H-1,2,3-triazol-4-yl]benzylidene}  
 7 indolin-2-one (**13i**)

8 Orange powder, yield: 60.19%, mp: 227°C. FI-IR (KBr,  $\nu_{\max}$   $\text{cm}^{-1}$ ):  
 9 3430 (NH), 1685 (C=O).  $^1\text{H}$  NMR (500 MHz, DMSO- $d_6$ )  $\delta$  10.66 (s, 1H,  
 10 N-H), 9.48 (s, 1H, H-triazole), 8.53 (d,  $J = 8.0$  Hz, 2H, Ar-H), 8.10 (s, 1H,  
 11 Ar-H), 8.00 (dd,  $J = 18.4, 8.0$  Hz, 3H, Ar-H), 7.84 (s, 1H, H-vinyllic), 7.72  
 12 (d,  $J = 7.6$  Hz, 1H, Ar-H), 7.68 (t,  $J = 8.1$  Hz, 1H, Ar-H), 7.60 (d,  $J = 8.0$   
 13 Hz, 1H, Ar-H), 7.22 (t,  $J = 7.5$  Hz, 1H, Ar-H), 7.00 (t,  $J = 7.3$  Hz, 1H,  
 14 Ar-H), 6.84 (d,  $J = 7.6$  Hz, 1H, Ar-H).  $^{13}\text{C}$  NMR (126 MHz, DMSO- $d_6$ )  $\delta$   
 15 166.97 (C=O), 146.80 (C-triazole), 140.68, 137.46 (C-vinyllic), 135.80,  
 16 134.10, 133.79, 132.53 (2C), 131.55, 131.42 (C-triazole), 128.89, 128.44,  
 17 126.80, 124.77 (3C), 120.93, 120.42 (C-vinyllic), 119.71, 119.67, 118.50,  
 18 109.23. ESI-HRMS calcd for  $C_{23}H_{16}ClN_4O$   $[M+H]^+$  399.0934, found:  
 19 399.1000.

20 4.1.7.10. (Z)-3-{4-[1-(4-chlorophenyl)-1H-1,2,3-triazol-4-yl]benzylidene}  
 21 indolin-2-one (**13j**)

22 Yellow powder, yield: 59.06%, mp: 235°C. FI-IR (KBr,  $\nu_{\max}$   $\text{cm}^{-1}$ ):



3432 (NH), 1689 (C=O).  $^1\text{H}$  NMR (500 MHz, DMSO- $d_6$ )  $\delta$  10.66 (s, 1H, N-H), 9.45 (s, 1H, H-triazole), 8.53 (d,  $J = 7.9$  Hz, 2H, Ar-H), 8.02 (t,  $J = 8.4$  Hz, 4H, Ar-H), 7.84 (s, 1H, H-vinyl), 7.74 (d,  $J = 7.7$  Hz, 3H, Ar-H), 7.22 (t,  $J = 7.4$  Hz, 1H, Ar-H), 7.01 (t,  $J = 7.4$  Hz, 1H, Ar-H), 6.84 (d,  $J = 7.6$  Hz, 1H, Ar-H).  $^{13}\text{C}$  NMR (126 MHz, DMSO- $d_6$ )  $\delta$  166.98 (C=O), 146.81 (C-triazole), 140.67, 135.83 (C-vinyl), 135.23, 133.76, 132.95, 132.53 (2C), 131.49 (C-triazole), 129.80 (2C), 128.89, 126.78, 125.61, 124.78 (2C), 121.61 (2C), 120.94, 120.33 (C-vinyl), 119.68, 109.23. ESI-HRMS calcd for  $\text{C}_{23}\text{H}_{16}\text{ClN}_4\text{O}$   $[\text{M}+\text{H}]^+$  399.0934, found: 399.1018.

#### 4.1.7.11.

(*Z*)-2-(4-{4-[(2-oxoindolin-3-ylidene)methyl]phenyl}-1*H*-1,2,3-triazol-1-yl)benzonitrile (**13k**)

Brown powder, yield: 49.58%, mp: 239 °C. FI-IR (KBr,  $\nu_{\text{max}}$   $\text{cm}^{-1}$ ): 3432 (NH), 1693 (C=O).  $^1\text{H}$  NMR (500 MHz, DMSO- $d_6$ )  $\delta$  10.65 (s, 1H, N-H), 9.36 (s, 1H, H-triazole), 8.20 (d,  $J = 7.8$  Hz, 1H, Ar-H), 8.12 (d,  $J = 7.7$  Hz, 2H, Ar-H), 8.06 – 7.96 (m, 2H, Ar-H), 7.88 (d,  $J = 7.8$  Hz, 2H, Ar-H), 7.82 (t,  $J = 7.5$  Hz, 1H, H-vinyl), 7.67 (s, 1H, Ar-H), 7.62 (d,  $J = 7.7$  Hz, 1H, Ar-H), 7.25 (t,  $J = 7.6$  Hz, 1H, Ar-H), 6.88 (t,  $J = 7.7$  Hz, 2H, Ar-H).  $^{13}\text{C}$  NMR (126 MHz, DMSO- $d_6$ )  $\delta$  168.47 (C=O), 146.49 (C-triazole), 142.91, 137.65 (C-vinyl), 134.95, 134.74, 134.65, 134.39, 132.55 (C-triazole), 130.76, 130.29, 130.06 (2C), 127.73, 125.56, 125.52 (2C), 122.90, 122.38, 121.04, 120.74 (C-vinyl), 115.62, 110.02, 106.97.

ESI-HRMS calcd for C<sub>24</sub>H<sub>16</sub>N<sub>5</sub>O [M+H]<sup>+</sup> 390.1277, found: 390.1349.

4.1.7.12.

(Z)-3-(4-{4-[(2-oxoindolin-3-ylidene)methyl]phenyl}-1H-1,2,3-triazol-1-yl)benzonitrile (**13l**)

Yellow powder, yield: 60.12%, mp: 240°C. FI-IR (KBr,  $\nu_{\max}$  cm<sup>-1</sup>): 3433 (NH), 1696 (C=O). <sup>1</sup>H NMR (500 MHz, DMSO-*d*<sub>6</sub>)  $\delta$  10.62 (s, 1H, N-H), 9.52 (s, 1H, H-triazole), 8.49 (s, 1H, Ar-H), 8.35 (d, *J* = 8.2 Hz, 1H, Ar-H), 8.07 (d, *J* = 8.0 Hz, 2H, Ar-H), 8.01 (d, *J* = 7.7 Hz, 1H, Ar-H), 7.87 (d, *J* = 7.5 Hz, 3H, H-vinylic, Ar-H), 7.66 (s, 1H, Ar-H), 7.62 (d, *J* = 7.7 Hz, 1H, Ar-H), 7.25 (t, *J* = 7.7 Hz, 1H, Ar-H), 6.88 (t, *J* = 7.9 Hz, 2H, Ar-H). <sup>13</sup>C NMR (126 MHz, DMSO-*d*<sub>6</sub>)  $\delta$  168.46 (C=O), 146.85 (C-triazole), 142.92, 136.87 (C-vinylic), 134.93, 134.33, 132.53, 132.18, 131.24 (C-triazole), 130.06 (2C), 127.71, 125.41 (2C), 124.79, 124.49, 123.26, 122.36, 121.02, 120.74, 120.38 (C-vinylic), 117.62, 112.74, 110.02. ESI-HRMS calcd for C<sub>24</sub>H<sub>16</sub>N<sub>5</sub>O [M+H]<sup>+</sup> 390.1277, found: 390.1355.

4.1.7.13.

(Z/E)-4-(4-{4-[(2-oxoindolin-3-ylidene)methyl]phenyl}-1H-1,2,3-triazol-1-yl)benzonitrile (**13m**)

Yellow powder, yield: 53.41%, mp: 241°C. FI-IR (KBr,  $\nu_{\max}$  cm<sup>-1</sup>): 3430 (NH), 1684 (C=O). <sup>1</sup>H NMR (500 MHz, DMSO-*d*<sub>6</sub>)  $\delta$  10.63 (s, 1H, N-H), 9.56 (s, 0.3H, H-triazole), 9.53 (s, 0.7H, H-triazole), 8.52 (d, *J* =

7.8 Hz, 1.3H, Ar-H), 8.20 (d,  $J = 7.7$  Hz, 2H, Ar-H), 8.14 (d,  $J = 8.3$  Hz, 2H, Ar-H), 8.08 (d,  $J = 7.6$  Hz, 0.7H, Ar-H), 8.02 (d,  $J = 7.9$  Hz, 1.3H, Ar-H), 7.86 (d,  $J = 7.7$  Hz, 0.6H, H-vinylic, Ar-H), 7.82 (s, 0.7H, H-vinylic), 7.71 (d,  $J = 7.4$  Hz, 0.7H, Ar-H), 7.65 (s, 0.3H, Ar-H), 7.61 (d,  $J = 7.7$  Hz, 0.3H, Ar-H), 7.23 (q,  $J = 9.2, 7.6$  Hz, 1H, Ar-H), 7.00 (t,  $J = 7.4$  Hz, 0.7H, Ar-H), 6.89 (d,  $J = 8.0$  Hz, 0.7H, Ar-H), 6.84 (d,  $J = 7.7$  Hz, 0.7H, Ar-H). ESI-HRMS calcd for  $C_{24}H_{16}N_5O$   $[M+H]^+$  390.1277, found: 390.1349.

#### 4.1.7.14.

(*Z*)-3-(4-{1-[4-chloro-3-(trifluoromethyl)phenyl]-1*H*-1,2,3-triazol-4-yl}benzylidene)indolin-2-one (**13n**)

Yellow powder, yield: 63.92%, mp: 219°C. FI-IR (KBr,  $\nu_{\max}$   $\text{cm}^{-1}$ ): 3432 (NH), 1677 (C=O).  $^1\text{H}$  NMR (500 MHz,  $\text{DMSO}-d_6$ )  $\delta$  10.66 (s, 1H, N-H), 9.59 (d,  $J = 2.1$  Hz, 1H, H-triazole), 8.53 (d,  $J = 6.6$  Hz, 2H, Ar-H), 8.43 (s, 1H, Ar-H), 8.32 (d,  $J = 8.4$  Hz, 1H, Ar-H), 8.03 (t,  $J = 7.5$  Hz, 3H, Ar-H), 7.84 (s, 1H, H-vinylic), 7.72 (d,  $J = 6.5$  Hz, 1H, Ar-H), 7.22 (t,  $J = 6.5$  Hz, 1H, Ar-H), 7.00 (t,  $J = 6.4$  Hz, 1H, Ar-H), 6.83 (d,  $J = 6.1$  Hz, 1H, Ar-H).  $^{13}\text{C}$  NMR (126 MHz,  $\text{DMSO}-d_6$ )  $\delta$  166.94 (C=O), 146.98 (C-triazole), 140.67, 135.73 (C-vinylic), 135.37, 133.86, 133.26, 132.53 (2C), 131.23 (C-triazole), 130.06, 128.89, 127.81 (d,  $J = 31.6$  Hz, C-trifluoromethylphenyl), 126.84, 125.38, 125.06, 124.75 (d,  $J = 3.6$  Hz, 2C, C-trifluoromethylphenyl, Ar-C), 123.23, 120.92, 120.64 (C-vinylic),

1 119.67, 119.15 (d,  $J = 5.2$  Hz, C-trifluoromethylphenyl), 109.22.  
 2 ESI-HRMS calcd for  $C_{24}H_{15}ClF_3N_4O$   $[M+H]^+$  467.0808, found:  
 3 467.0887.

4 *4.1.7.15. (Z/E)-5-fluoro-3-[4-(1-phenyl-1H-1,2,3-triazol-4-yl)benzylidene]*  
 5 *indolin-2-one (14a)*

6 Orange powder, yield: 69.92%, mp: 229 °C. FI-IR (KBr,  $\nu_{\max}$   $\text{cm}^{-1}$ ):  
 7 3432 (NH), 1687 (C=O).  $^1\text{H}$  NMR (500 MHz, DMSO- $d_6$ )  $\delta$  10.67 (s, 1H,  
 8 N-H), 9.44 (s, 0.5H, H-triazole), 9.42 (s, 0.5H, H-triazole), 8.54 (d,  $J =$   
 9 7.8 Hz, 1H, Ar-H), 8.12 (d,  $J = 8.0$  Hz, 1H, Ar-H), 8.06 (d,  $J = 7.9$  Hz, 1H,  
 10 Ar-H), 7.97 (d,  $J = 7.6$  Hz, 2H, Ar-H), 7.92 (s, 0.5H, Ar-H), 7.86 (d,  $J =$   
 11 7.7 Hz, 1H, H-vinyl), 7.74 (s, 0.5H, Ar-H), 7.65 (t,  $J = 7.7$  Hz, 2.5H,  
 12 Ar-H), 7.53 (t,  $J = 7.4$  Hz, 1H, Ar-H), 7.33 (d,  $J = 9.0$  Hz, 0.5H, Ar-H),  
 13 7.11 (t,  $J = 9.0$  Hz, 0.5H, Ar-H), 7.05 (t,  $J = 9.1$  Hz, 0.5H, Ar-H), 6.88 (dd,  
 14  $J = 8.4, 4.5$  Hz, 0.5H, Ar-H), 6.81 (dd,  $J = 8.3, 4.3$  Hz, 0.5H, Ar-H).  
 15 ESI-HRMS calcd for  $C_{23}H_{16}FN_4O$   $[M+H]^+$  383.1230, found: 383.1313.

16 *4.1.7.16. (Z/E)-5-fluoro-3-{4-[1-(o-tolyl)-1H-1,2,3-triazol-4-yl]*  
 17 *benzylidene} indolin-2-one (14b)*

18 Yellow powder, yield: 55.15%, mp: 221 °C. FI-IR (KBr,  $\nu_{\max}$   $\text{cm}^{-1}$ ):  
 19 3432 (NH), 1701 (C=O).  $^1\text{H}$  NMR (500 MHz, DMSO- $d_6$ )  $\delta$  10.68 (s, 1H,  
 20 N-H), 9.09 (d,  $J = 1.1$  Hz, 1H, H-triazole), 8.54 (d,  $J = 8.2$  Hz, 1H, Ar-H),  
 21 8.12 (d,  $J = 8.0$  Hz, 1H, Ar-H), 8.06 (d,  $J = 8.2$  Hz, 1H, Ar-H), 7.93 (s,  
 22 0.4H, Ar-H), 7.85 (d,  $J = 8.0$  Hz, 1H, H-vinyl), 7.74 (s, 0.6H, Ar-H),

7.67 (d,  $J = 9.0$  Hz, 0.4H, Ar-H), 7.56 – 7.51 (m, 3H, Ar-H), 7.48 – 7.43 (m, 1H, Ar-H), 7.32 (d,  $J = 9.2$  Hz, 0.6H, Ar-H), 7.10 (t,  $J = 8.9$  Hz, 0.6H, Ar-H), 7.04 (t,  $J = 9.0$  Hz, 0.4H, Ar-H), 6.88 (dd,  $J = 8.0, 4.7$  Hz, 0.6H, Ar-H), 6.81 (dd,  $J = 7.8, 4.4$  Hz, 0.4H, Ar-H), 2.24 (s, 3H, CH<sub>3</sub>).

ESI-HRMS calcd for C<sub>24</sub>H<sub>18</sub>FN<sub>4</sub>O [M+H]<sup>+</sup> 397.1386, found: 397.1463.

4.1.7.17. (Z)-5-fluoro-3-{4-[1-(*m*-tolyl)-1H-1,2,3-triazol-4-yl]benzylidene} indolin-2-one (**14c**)

Orange powder, yield: 65.29%, mp: 217°C. FI-IR (KBr,  $\nu_{\max}$  cm<sup>-1</sup>): 3432 (NH), 1686 (C=O). <sup>1</sup>H NMR (500 MHz, DMSO-*d*<sub>6</sub>)  $\delta$  10.66 (s, 1H, N-H), 9.39 (s, 1H, H-triazole), 8.54 (d,  $J = 8.0$  Hz, 2H, Ar-H), 8.05 (d,  $J = 8.0$  Hz, 2H, Ar-H), 7.92 (s, 1H, Ar-H), 7.81 (s, 1H, H-vinyl), 7.75 (d,  $J = 8.2$  Hz, 1H, Ar-H), 7.66 (d,  $J = 9.3$  Hz, 1H, Ar-H), 7.52 (t,  $J = 7.8$  Hz, 1H, Ar-H), 7.34 (d,  $J = 7.6$  Hz, 1H, Ar-H), 7.05 (t,  $J = 9.4$  Hz, 1H, Ar-H), 6.81 (dd,  $J = 8.6, 4.4$  Hz, 1H, Ar-H), 2.45 (s, 3H, CH<sub>3</sub>). <sup>13</sup>C NMR (126 MHz, DMSO-*d*<sub>6</sub>)  $\delta$  166.99 (C=O), 158.74, 156.87, 146.52 (C-triazole), 139.55, 137.61 (C-vinyl), 136.85, 136.37, 133.39, 132.75 (2C), 132.08 (C-triazole), 129.58, 129.25, 126.31 (d,  $J = 8.6$  Hz, C-fluorobenzene), 124.79 (2C, C-vinyl, Ar-C), 120.30 (d,  $J = 6.3$  Hz, C-fluorobenzene), 117.03, 114.98 (d,  $J = 24.0$  Hz, C-fluorobenzene), 109.94 (d,  $J = 8.3$  Hz, C-fluorobenzene), 107.20, 107.00, 20.79 (CH<sub>3</sub>). ESI-HRMS calcd for C<sub>24</sub>H<sub>18</sub>FN<sub>4</sub>O [M+H]<sup>+</sup> 397.1386, found: 397.1460.

4.1.7.18. (Z)-5-fluoro-3-{4-[1-(*p*-tolyl)-1H-1,2,3-triazol-4-yl]benzylidene}

*indolin-2-one (14d)*

Orange powder, yield: 56.25%, mp: 204 °C. FI-IR (KBr,  $\nu_{\max}$  cm<sup>-1</sup>): 3433 (NH), 1683 (C=O). <sup>1</sup>H NMR (500 MHz, DMSO-*d*<sub>6</sub>)  $\delta$  10.67 (s, 1H, N-H), 9.36 (s, 1H, H-triazole), 8.54 (d, *J* = 7.9 Hz, 2H, Ar-H), 8.05 (d, *J* = 7.8 Hz, 2H, Ar-H), 7.92 (s, 1H, Ar-H), 7.84 (d, *J* = 7.6 Hz, 2H, H-vinyl, Ar-H), 7.67 (d, *J* = 9.0 Hz, 1H, Ar-H), 7.45 (d, *J* = 7.8 Hz, 2H, Ar-H), 7.05 (t, *J* = 9.1 Hz, 1H, Ar-H), 6.81 (dd, *J* = 7.8, 4.2 Hz, 1H, Ar-H), 2.40 (s, 3H, CH<sub>3</sub>). <sup>13</sup>C NMR (126 MHz, DMSO-*d*<sub>6</sub>)  $\delta$  167.01 (C=O), 158.76, 156.89, 146.50 (C-triazole), 138.35, 137.65, 136.86 (C-vinyl), 134.19, 133.38, 132.76 (2C), 132.13 (C-triazole), 130.14 (2C), 126.35 (d, *J* = 3.4 Hz, C-fluorobenzene), 124.80 (2C), 120.22 (C-vinyl), 119.82 (2C), 114.99 (d, *J* = 24.1 Hz, C-fluorobenzene), 109.96 (d, *J* = 8.1 Hz, C-fluorobenzene), 107.12 (d, *J* = 25.4 Hz, C-fluorobenzene), 20.44 (CH<sub>3</sub>). ESI-HRMS calcd for C<sub>24</sub>H<sub>18</sub>FN<sub>4</sub>O [M+H]<sup>+</sup> 397.1386, found: 397.1464.

*4.1.7.19.*

*(Z)-5-fluoro-3-{4-[1-(2-fluorophenyl)-1H-1,2,3-triazol-4-yl]benzylidene}indolin-2-one (14e)*

Yellow powder, yield: 64.18%, mp: 248 °C. FI-IR (KBr,  $\nu_{\max}$  cm<sup>-1</sup>): 3432 (NH), 1699 (C=O). <sup>1</sup>H NMR (500 MHz, DMSO-*d*<sub>6</sub>)  $\delta$  10.66 (s, 1H, N-H), 9.21 (s, 1H, H-triazole), 8.14 (d, *J* = 7.9 Hz, 2H, Ar-H), 7.93 (t, *J* = 7.6 Hz, 1H, Ar-H), 7.84 (d, *J* = 7.8 Hz, 2H, H-vinyl, Ar-H), 7.73 (s, 1H, Ar-H), 7.68 – 7.58 (m, 2H, Ar-H), 7.48 (t, *J* = 7.4 Hz, 1H, Ar-H), 7.31 (d,

$J = 9.0$  Hz, 1H, Ar-H), 7.09 (t,  $J = 8.6$  Hz, 1H, Ar-H), 6.90 – 6.84 (m, 1H, Ar-H).  $^{13}\text{C}$  NMR (126 MHz, DMSO- $d_6$ )  $\delta$  168.44 (C=O), 157.95, 156.08, 154.71, 152.71, 146.14 (C-triazole), 139.21, 136.73 (C-vinylic), 133.72, 131.34 (C-triazole), 130.03 (2C), 127.32 (d,  $J = 2.7$  Hz, C-fluorobenzene), 125.83, 125.57 (2C, C-vinylic, Ar-C), 125.45 (d,  $J = 3.5$  Hz, C-fluorobenzene), 123.38 (d,  $J = 4.2$  Hz, C-fluorobenzene), 121.68 (d,  $J = 8.7$  Hz, C-fluorobenzene), 117.06 (d,  $J = 19.4$  Hz, C-fluorobenzene), 116.41, 110.68 (d,  $J = 8.4$  Hz, C-fluorobenzene), 109.23. ESI-HRMS calcd for  $\text{C}_{23}\text{H}_{15}\text{F}_2\text{N}_4\text{O}$   $[\text{M}+\text{H}]^+$  401.1136, found: 401.1201.

4.1.7.20.

*(Z)-5-fluoro-3-{4-[1-(3-fluorophenyl)-1H-1,2,3-triazol-4-yl]benzylidene}indolin-2-one (14f)*

Orange powder, yield: 51.56%, mp: 241 °C. FI-IR (KBr,  $\nu_{\text{max}}$   $\text{cm}^{-1}$ ): 3432 (NH), 1685 (C=O).  $^1\text{H}$  NMR (500 MHz, DMSO- $d_6$ )  $\delta$  10.65 (s, 1H, N-H), 9.45 (s, 1H, H-triazole), 8.53 (d,  $J = 8.1$  Hz, 2H, Ar-H), 8.03 (d,  $J = 8.2$  Hz, 2H, Ar-H), 7.93 – 7.82 (m, 3H, H-vinylic, Ar-H), 7.74 – 7.62 (m, 2H, Ar-H), 7.39 (t,  $J = 8.5$  Hz, 1H, Ar-H), 7.04 (t,  $J = 8.9$  Hz, 1H, Ar-H), 6.81 (dd,  $J = 8.1, 4.4$  Hz, 1H, Ar-H).  $^{13}\text{C}$  NMR (126 MHz, DMSO- $d_6$ )  $\delta$  168.43 (C=O), 163.27, 161.32, 156.08, 146.62 (C-triazole), 139.23, 137.63 (d,  $J = 10.4$  Hz, C-fluorobenzene), 136.70 (C-vinylic), 133.76, 132.75, 131.78 (d,  $J = 9.3$  Hz, C-fluorobenzene), 131.34 (C-triazole), 130.08 (2C), 127.35 (d,  $J = 2.8$  Hz, C-fluorobenzene), 125.47 (2C),

1 124.83 (C-vinyl), 120.46 (d,  $J = 8.8$  Hz, C-fluorobenzene), 116.34 (d,  $J$   
 2  $= 23.6$  Hz, C-fluorobenzene), 115.80 (d,  $J = 2.9$  Hz, C-fluorobenzene),  
 3 110.70 (d,  $J = 8.1$  Hz, C-fluorobenzene), 107.50 (d,  $J = 3.8$  Hz,  
 4 C-fluorobenzene). ESI-HRMS calcd for  $C_{23}H_{15}F_2N_4O$   $[M+H]^+$  401.1136,  
 5 found: 401.1212.

6 4.1.7.21.

7 (Z)-5-fluoro-3-{4-[1-(4-fluorophenyl)-1H-1,2,3-triazol-4-yl]benzylidene}i  
 8 ndolin-2-one (**14g**)

9 Orange powder, yield: 66.81%, mp: 252°C. FI-IR (KBr,  $\nu_{\max}$   $\text{cm}^{-1}$ ):  
 10 3440 (NH), 1689 (C=O).  $^1\text{H}$  NMR (500 MHz,  $\text{DMSO}-d_6$ )  $\delta$  10.66 (s, 1H,  
 11 N-H), 9.36 (s, 1H, H-triazole), 8.52 (d,  $J = 8.1$  Hz, 2H, Ar-H), 8.04 – 7.97  
 12 (m, 4H, Ar-H), 7.88 (s, 1H, H-vinyl), 7.64 (d,  $J = 8.5$  Hz, 1H, Ar-H),  
 13 7.49 (t,  $J = 8.5$  Hz, 2H, Ar-H), 7.03 (t,  $J = 8.8$  Hz, 1H, Ar-H), 6.80 (dd,  $J$   
 14  $= 8.2, 4.3$  Hz, 1H, Ar-H).  $^{13}\text{C}$  NMR (126 MHz,  $\text{DMSO}-d_6$ )  $\delta$  167.00  
 15 (C=O), 162.54, 160.59, 158.74, 156.87, 146.62 (C-triazole), 137.56,  
 16 136.84 (C-vinyl), 133.42, 132.96 (d,  $J = 2.8$  Hz, C-fluorobenzene),  
 17 132.74 (2C), 131.95 (C-triazole), 126.36 (d,  $J = 3.7$  Hz, C-fluorobenzene),  
 18 124.78 (2C), 122.25 (d,  $J = 9.0$  Hz, C-fluorobenzene), 120.53 (C-vinyl),  
 19 116.62 (d,  $J = 23.1$  Hz, 2C, C-fluorobenzene), 114.95 (d,  $J = 23.8$  Hz,  
 20 C-fluorobenzene), 109.92 (d,  $J = 8.3$  Hz, C-fluorobenzene), 107.09 (d,  $J$   
 21  $= 25.4$  Hz, C-fluorobenzene). ESI-HRMS calcd for  $C_{23}H_{15}F_2N_4O$   $[M+H]^+$   
 22 401.1208, found: 401.1215.



## 4.1.7.22.

(*Z*)-3-{4-[1-(2-chlorophenyl)-1*H*-1,2,3-triazol-4-yl]benzylidene}-5-fluoroin-  
 ndolin-2-one (**14h**)

Yellow powder, yield 57.36%, mp: 235°C. FI-IR (KBr,  $\nu_{\max}$  cm<sup>-1</sup>): 3432 (NH), 1708 (C=O). <sup>1</sup>H NMR (500 MHz, DMSO-*d*<sub>6</sub>)  $\delta$  10.68 (s, 1H, N-H), 9.19 (s, 1H, H-triazole), 8.13 (d, *J* = 7.8 Hz, 2H, Ar-H), 7.89 – 7.78 (m, 4H, H-vinyl, Ar-H), 7.74 (s, 1H, Ar-H), 7.71 – 7.61 (m, 2H, Ar-H), 7.32 (d, *J* = 9.1 Hz, 1H, Ar-H), 7.10 (t, *J* = 8.7 Hz, 1H, Ar-H), 6.88 (dd, *J* = 8.0, 4.5 Hz, 1H, Ar-H). <sup>13</sup>C NMR (126 MHz, DMSO-*d*<sub>6</sub>)  $\delta$  168.44 (C=O), 157.96, 156.08, 145.73 (C-triazole), 139.21, 136.77 (C-vinyl), 134.29, 133.67, 131.70, 131.45, 130.46 (C-triazole), 130.07 (2C), 128.47, 128.33 (d, *J* = 14.0 Hz, C-fluorobenzene), 127.32 (d, *J* = 3.0 Hz, C-fluorobenzene), 125.49 (2C), 124.20 (C-vinyl), 121.69 (d, *J* = 8.7 Hz, C-fluorobenzene), 116.34 (d, *J* = 23.8 Hz, C-fluorobenzene), 110.70 (d, *J* = 8.4 Hz, C-fluorobenzene), 109.33 (d, *J* = 25.7 Hz, C-fluorobenzene). ESI-HRMS calcd for C<sub>23</sub>H<sub>15</sub>ClFN<sub>4</sub>O [M+H]<sup>+</sup> 417.0840, found: 417.0921.

## 4.1.7.23.

(*Z*)-3-{4-[1-(3-chlorophenyl)-1*H*-1,2,3-triazol-4-yl]benzylidene}-5-fluoroin-  
 ndolin-2-one (**14i**)

Orange powder, yield: 64.52%, mp: 248°C. FI-IR (KBr,  $\nu_{\max}$  cm<sup>-1</sup>): 3432 (NH), 1685 (C=O). <sup>1</sup>H NMR (500 MHz, DMSO-*d*<sub>6</sub>)  $\delta$  10.66 (s, 1H, N-H), 9.47 (s, 1H, H-triazole), 8.53 (d, *J* = 8.0 Hz, 2H, Ar-H), 8.08 (s, 1H,

1 Ar-H), 8.02 (d,  $J = 8.0$  Hz, 2H, Ar-H), 7.97 (d,  $J = 8.1$  Hz, 1H, Ar-H),  
 2 7.90 (s, 1H, H-vinylic), 7.66 (q,  $J = 7.9$  Hz, 2H, Ar-H), 7.59 (d,  $J = 8.0$   
 3 Hz, 1H, Ar-H), 7.04 (t,  $J = 9.0$  Hz, 1H, Ar-H), 6.80 (dd,  $J = 8.2, 4.3$  Hz,  
 4 1H, Ar-H).  $^{13}\text{C}$  NMR (126 MHz, DMSO- $d_6$ )  $\delta$  166.99 (C=O), 158.74,  
 5 156.88, 146.72 (C-triazole), 137.49 (d,  $J = 14.2$  Hz, C-fluorobenzene),  
 6 136.87 (C-vinylic), 134.10, 133.52, 132.76 (2C), 131.79, 131.53  
 7 (C-triazole), 128.44, 126.44 (d,  $J = 2.9$  Hz, C-fluorobenzene), 126.29 (d,  
 8  $J = 8.9$  Hz, C-fluorobenzene), 124.81 (2C), 120.49 (C-vinylic), 119.68,  
 9 118.47, 115.00 (d,  $J = 23.9$  Hz, C-fluorobenzene), 109.95 (d,  $J = 8.1$  Hz,  
 10 C-fluorobenzene), 107.12 (d,  $J = 25.4$  Hz, C-fluorobenzene). ESI-HRMS  
 11 calcd for  $\text{C}_{23}\text{H}_{15}\text{ClFN}_4\text{O}$   $[\text{M}+\text{H}]^+$  417.0840, found: 417.0914.

12 4.1.7.24.

13 (*Z/E*)-3-{4-[1-(4-chlorophenyl)-1*H*-1,2,3-triazol-4-yl]benzylidene}-5-fluo  
 14 roindolin-2-one (**14j**)

15 Orange powder, yield: 48.67%, mp: 233 °C. FI-IR (KBr,  $\nu_{\text{max}}$   $\text{cm}^{-1}$ ):  
 16 3439 (NH), 1687 (C=O).  $^1\text{H}$  NMR (500 MHz, DMSO- $d_6$ )  $\delta$  10.67 (s, 1H,  
 17 N-H), 9.45 (d,  $J = 11.2$  Hz, 1H, H-triazole), 8.53 (d,  $J = 8.3$  Hz, 1H,  
 18 Ar-H), 8.10 (d,  $J = 8.6$  Hz, 1H, Ar-H), 8.02 (dd,  $J = 14.0, 8.5$  Hz, 3H,  
 19 Ar-H), 7.91 (s, 0.5H, Ar-H), 7.86 (d,  $J = 8.0$  Hz, 1H, H-vinylic), 7.73 (d,  $J$   
 20 = 7.4 Hz, 2.5H, Ar-H), 7.66 (d,  $J = 9.0$  Hz, 0.5H, Ar-H), 7.31 (d,  $J = 9.2$   
 21 Hz, 0.5H, Ar-H), 7.11 (t,  $J = 8.8$  Hz, 0.5H, Ar-H), 7.04 (t,  $J = 8.9$  Hz,  
 22 0.5H, Ar-H), 6.88 (dd,  $J = 8.4, 4.6$  Hz, 0.5H, Ar-H), 6.81 (dd,  $J = 8.3, 4.3$

1 Hz, 0.5H, Ar-H). ESI-HRMS calcd for  $C_{23}H_{15}ClFN_4O$   $[M+H]^+$  417.0840,  
 2 found: 417.0909.

3 4.1.7.25.

4 (Z/E)-2-(4-{4-[(5-fluoro-2-oxoindolin-3-ylidene)methyl]phenyl}-1H-1,2,3  
 5 -triazol-1-yl)benzonitrile (**14k**)

6 Brown powder, yield: 58.26%, mp: 218 °C. FI-IR (KBr,  $\nu_{\max}$   $cm^{-1}$ ): 3439  
 7 (NH), 1690 (C=O).  $^1H$  NMR (500 MHz, DMSO- $d_6$ )  $\delta$  10.68 (s, 1H, N-H),  
 8 9.36 (s, 1H, H-triazole), 8.55 (d,  $J = 7.7$  Hz, 1.7H, Ar-H), 8.19 (d,  $J = 7.2$   
 9 Hz, 1H, Ar-H), 8.14 (d,  $J = 7.2$  Hz, 0.3H, Ar-H), 8.07 (d,  $J = 7.6$  Hz, 1.7H,  
 10 Ar-H), 7.99 (t,  $J = 9.3$  Hz, 2H, Ar-H), 7.93 (s, 0.8H, Ar-H), 7.88 (d,  $J =$   
 11 6.8 Hz, 0.3H, Ar-H), 7.81 (t,  $J = 6.7$  Hz, 1H, H-vinyl), 7.74 (s, 0.2H,  
 12 Ar-H), 7.67 (d,  $J = 8.4$  Hz, 0.8H, Ar-H), 7.32 (d,  $J = 8.8$  Hz, 0.2H, Ar-H),  
 13 7.10 (d,  $J = 8.7$  Hz, 0.2H, Ar-H), 7.05 (t,  $J = 8.8$  Hz, 0.8H, Ar-H), 6.88 (s,  
 14 0.2H, Ar-H), 6.81 (d,  $J = 4.6$  Hz, 0.8H, Ar-H). ESI-HRMS calcd for  
 15  $C_{24}H_{15}FN_5O$   $[M+H]^+$  408.1182, found: 408.1260.

16 4.1.7.26.

17 (Z)-3-(4-{4-[(5-fluoro-2-oxoindolin-3-ylidene)methyl]phenyl}-1H-1,2,3-tr  
 18 iazol-1-yl)benzonitrile (**14l**)

19 Yellow powder, yield: 63.43%, mp: 246 °C. FI-IR (KBr,  $\nu_{\max}$   $cm^{-1}$ ):  
 20 3430 (NH), 1679 (C=O).  $^1H$  NMR (500 MHz, DMSO- $d_6$ )  $\delta$  10.68 (s, 1H,  
 21 N-H), 9.53 (s, 1H, H-triazole), 8.54 (d,  $J = 7.9$  Hz, 2H, Ar-H), 8.49 (s, 1H,  
 22 Ar-H), 8.35 (d,  $J = 8.3$  Hz, 1H, Ar-H), 8.02 (t,  $J = 7.6$  Hz, 3H, Ar-H), 7.92

(s, 1H, Ar-H), 7.87 (t,  $J = 8.0$  Hz, 1H, H-vinyl), 7.67 (d,  $J = 8.8$  Hz, 1H, Ar-H), 7.05 (t,  $J = 9.0$  Hz, 1H, Ar-H), 6.81 (dd,  $J = 8.3, 4.3$  Hz, 1H, Ar-H).  $^{13}\text{C}$  NMR (126 MHz, DMSO- $d_6$ )  $\delta$  166.99 (C=O), 158.75, 156.88, 146.85 (C-triazole), 137.52, 136.83 (C-vinyl), 133.61, 132.79 (2C), 132.23, 131.68, 131.25 (C-triazole), 130.27, 126.52 (d,  $J = 3.2$  Hz, C-fluorobenzene), 124.84 (2C), 124.55, 123.31, 120.62 (C-vinyl), 117.64, 115.05 (d,  $J = 24.3$  Hz, C-fluorobenzene), 112.71, 109.98 (d,  $J = 8.3$  Hz, C-fluorobenzene), 107.16 (d,  $J = 25.4$  Hz, C-fluorobenzene). ESI-HRMS calcd for  $\text{C}_{24}\text{H}_{15}\text{FN}_5\text{O}$   $[\text{M}+\text{H}]^+$  408.1182, found: 408.1265.

#### 4.1.7.27.

(*Z/E*)-4-(4-{4-[(5-fluoro-2-oxoindolin-3-ylidene)methyl]phenyl}-1*H*-1,2,3-triazol-1-yl)benzonitrile (**14m**)

Yellow powder, yield: 59.91%, mp: 215°C. FI-IR (KBr,  $\nu_{\text{max}}$   $\text{cm}^{-1}$ ): 3432 (NH), 1684 (C=O).  $^1\text{H}$  NMR (500 MHz, DMSO- $d_6$ )  $\delta$  10.68 (s, 1H, N-H), 9.10 (s, 1H, H-triazole), 8.54 (d,  $J = 8.2$  Hz, 1H, Ar-H), 8.12 (d,  $J = 8.0$  Hz, 1H, Ar-H), 8.06 (d,  $J = 8.2$  Hz, 1H, Ar-H), 7.93 (s, 0.4H, Ar-H), 7.85 (d,  $J = 7.9$  Hz, 1H, H-vinyl), 7.74 (s, 0.6H, Ar-H), 7.67 (d,  $J = 8.8$  Hz, 0.4H, Ar-H), 7.56 – 7.50 (m, 3H, Ar-H), 7.46 (s, 1H, Ar-H), 7.32 (d,  $J = 9.2$  Hz, 0.6H, Ar-H), 7.11 (t,  $J = 8.8$  Hz, 0.6H, Ar-H), 7.05 (t,  $J = 8.9$  Hz, 0.4H, Ar-H), 6.88 (dd,  $J = 8.3, 4.6$  Hz, 0.6H, Ar-H), 6.81 (dd,  $J = 8.3, 4.3$  Hz, 0.4H, Ar-H). ESI-HRMS calcd for  $\text{C}_{24}\text{H}_{15}\text{FN}_5\text{O}$   $[\text{M}+\text{H}]^+$  408.1182, found: 408.1259.

#### 4.1.7.28.

(Z)-3-(4-{1-[4-chloro-3-(trifluoromethyl)phenyl]-1H-1,2,3-triazol-4-yl}benzylidene)-5-fluoroindolin-2-one (**14n**)

Orange powder, yield: 47.50%, mp: 251 °C. FI-IR (KBr,  $\nu_{\max}$  cm<sup>-1</sup>): 3432 (NH), 1684 (C=O). <sup>1</sup>H NMR (500 MHz, DMSO-*d*<sub>6</sub>)  $\delta$  10.66 (s, 1H, N-H), 9.58 (s, 1H, H-triazole), 8.52 (d, *J* = 7.5 Hz, 2H, Ar-H), 8.41 (s, 1H, Ar-H), 8.31 (d, *J* = 8.7 Hz, 1H, Ar-H), 8.01 (d, *J* = 6.9 Hz, 3H, Ar-H), 7.89 (s, 1H, H-vinyl), 7.64 (d, *J* = 8.7 Hz, 1H, Ar-H), 7.03 (t, *J* = 8.8 Hz, 1H, Ar-H), 6.80 (s, 1H, Ar-H). <sup>13</sup>C NMR (126 MHz, DMSO-*d*<sub>6</sub>)  $\delta$  166.96 (C=O), 158.73, 156.86, 146.91 (C-triazole), 137.48, 136.87 (C-vinyl), 135.35, 133.60, 133.01 (d, *J* = 64.2 Hz, 2C, C-trifluoromethylphenyl), 131.61 (C-triazole), 130.30, 127.81 (d, *J* = 31.7 Hz, C-trifluoromethylphenyl), 126.49 (d, *J* = 3.0 Hz, C-trifluoromethylphenyl), 126.26 (d, *J* = 8.8 Hz, C-trifluoromethylphenyl), 124.94 (d, *J* = 29.6 Hz, 2C, C-fluorobenzene, C-trifluoromethylphenyl), 123.23, 121.06, 120.73 (C-vinyl), 119.15 (d, *J* = 5.5 Hz, C-fluorobenzene), 115.03 (d, *J* = 24.0 Hz, C-fluorobenzene), 109.96 (d, *J* = 8.4 Hz, C-fluorobenzene), 107.13 (d, *J* = 25.1 Hz, C-fluorobenzene). ESI-HRMS calcd for C<sub>24</sub>H<sub>14</sub>ClF<sub>4</sub>N<sub>4</sub>O [M+H]<sup>+</sup> 485.0787, found: 485.0793.

#### 4.2. VEGFR-2 kinase assay in vitro

The ADP-Glo kinase assay kit (Promega, Madison) was used for VEGFR-2 kinase analysis. According to manufacturer's instructions, The

1 general procedure is as follows: 20  $\mu$ L mix VEGFR-2 kinase (Invitrogen,  
2 USA), 30  $\mu$ L substrate (ADP-Glo, 50  $\mu$ M), 30  $\mu$ L ATP (50  $\mu$ M) and 20  
3  $\mu$ L different concentrations (0 nM, 25 nM, 50 nM, 100 nM, 200 nM) of  
4 test compounds, and the total volume in a 96-well light-proof microtiter  
5 plate are 100 $\mu$ L of final buffer. Incubate in liquid. Wells containing  
6 substrate and compound-free kinase were used as overall reaction  
7 controls. The assay plate was incubated at 37°C for 30 min in the dark.  
8 Use a full-wavelength microplate reader to perform detection at dual  
9 wavelengths to obtain fluorescence values, which are further used to  
10 calculate IC<sub>50</sub> values. The obtained data were compared with sunitinib as a  
11 standard inhibitor for VEGFR-2.

#### 12 *4.3. Cell culture and CCK-8 assay in vitro*

13 Human colon cancer (HT-29) cells, human gastric cancer (MKN-45)  
14 cells, human umbilical vein endothelial cells (HUVECs) were purchased  
15 from the China Cell Resource Bank and recorded as F0 generation cells.  
16 Standardized training according to the protocol provided by the supplier  
17 dilute fibronectin to 1 mg/mL with sterile water. Add 25 mL Fetal Bovine  
18 Serum (FBS), 5 mL Endothelial Cell Growth Supplement (ECGS), and 5  
19 mL P/S solution to 500 mL Endothelial Cell Medium (ECM) (ScienCell,  
20 SC-1001). These operations are protected from light. All compounds were  
21 dissolved in DMSO as a 1 mM stock solution. Further dilutions of all  
22 compounds were performed in DMEM (GIBCO, 21127-022) incomplete

1 medium. The compound was serially diluted to the final concentration:  
2 1.25  $\mu$ M, 2.5  $\mu$ M, 5  $\mu$ M, 10  $\mu$ M, 20  $\mu$ M. The concentration of DMSO is  
3 0.5% [47].

4 The antiproliferative activity was determined using the CCK-8 assay  
5 [48]. HT-29, MKN-45, and HUVECs of F4 generation were cultured in  
6 culture flasks. When the number of cells reached 80%, the cells were  
7 harvested and transferred to a 96-well plate (treated with fibronectin at a  
8 concentration of 2 mg/cm<sup>2</sup>) and cultured at 3000 cells per well overnight.  
9 ECM complete medium was aspirated in DMEM complete medium, and  
10 50 ng/mL VEGF was added. 100  $\mu$ L of the diluted compound was added  
11 to the corresponding experimental wells. The mixture was incubated for  
12 24 h, and 10  $\mu$ L of CCK-8 reagent was added to each well and incubated  
13 for 4h. The optical density (OD) of each well was detected at 490 nm.

#### 14 4.4. Transwell assay

15 A transwell chamber (pore size 8  $\mu$ m; Corning Costar, Cambridge,  
16 Massachusetts, USA) was used to measure the migration capacity of  
17 HUVEC. For transwell analysis, HUVECs were treated with serum-free  
18 DMEM medium containing different concentrations of compound **13d** (0  
19  $\mu$ M, 0.2  $\mu$ M, 0.4  $\mu$ M or 0.8  $\mu$ M) for 24 hours, and then collected and  
20 counted.  $1 \times 10^4$  HUVECs were inoculated into the upper chamber, and the  
21 lower chamber contained DMEM medium supplemented with 20% serum.  
22 After 24 hours of incubation, the filter was fixed in methanol and stained

with 0.1% crystal violet. Gently wipe the upper surface of the filter, image under the microscope, and count the total number of HUVECs that have migrated through the filter's lower surface [49].

#### 4.5. Tube formation

After treated with different concentrations (0  $\mu$ M, 0.2  $\mu$ M, 0.4  $\mu$ M or 0.8  $\mu$ M) of compound **13d**, the HUVECs were collected.  $1 \times 10^4$  cells HUVECs were seeded on Matrigel's surface (#354234, Corning, USA), then cultured for 6 hours. The tube formation was then observed and photographed with a microscope. Use image pro plus software to calculate the total length of tubes.

#### 4.6 Western blot analysis

HUVECs were treated with different concentrations (0  $\mu$ M, 0.2  $\mu$ M, 0.4  $\mu$ M or 0.8  $\mu$ M) of compound **13d** for 24 hours. Primary antibody (100  $\mu$ L/cm<sup>2</sup>): VEGFR-2 (26415-1-AP, Proteintech Group), p-VEGFR-2 (Tyr951) (#2471, Cell Signaling Technology). The cellular level of protein was determined by standard western blotting.

#### 4.7. Zebrafish labeling and culture

The research group cooperated with China Zebrafish Resource Center (CZRC) to construct a blood vessel marker zebrafish (Tg(kdrl:EGFP)) with a genotype of s843Tg/+, which was recorded as the F0 generation. Collect the fish eggs of the F2 generation, and add different concentrations of target compounds to the culture solution after 24 hours



to make the final concentration of the culture solution 40 mg/L. After 24 hours of action, the zebrafish were anesthetized *in vivo*, and the internode angiogenesis and sprouting were observed under a confocal microscope.

#### 4.8. Molecular docking study

Molecular docking study was carried out with MOE (Molecular Operating Environment, version 2016.08, Chemical Computing Group Inc., Canada) [50]. Two mol2 format files of compound **13d** and sunitinib were subjected to energy minimization with Amber10: EHT force-field in MOE. The crystal structure of VEGFR-2 in complex with sunitinib (PDB ID: 4AGD) was downloaded from Protein Data Bank (<https://www.rcsb.org/>) and successively optimized with Structure Preparation and Protonate 3D [51]. The ligand atoms were chosen as the docking site in the docking procedure, which was conducted with default parameters.

#### 4.9. Molecular dynamics (MD) simulations

MD simulations of two systems in PDB format were conducted using NAMD software (version 2.14), and configuration files were generated in VMD (visual molecular dynamics) [52]. Energy minimization and equilibration with Gasteiger–Huckel charges used Boltzmann's initial velocity in CHARMM 22 force field file, which performed in a 15 Å<sup>3</sup> size water box. Ultimately, 10 ns MD simulations for three proteins at constant temperature (300 K) and pressure (1 atm) were carried out to

1 analyze three systems' binding affinity and stability.

## 2 **Acknowledgments**

3 This work was financial support for this work from the National  
4 Natural Science Foundation of China (No.81573687), and the project of  
5 Liaoning distinguished professor, China. The key research and  
6 development project of Liaoning Province ("The research and  
7 development of the multi-target anti-tumor drug candidate HXA-20"  
8 2019 No. 26).

9 At the same time, we are very grateful to the key special project of the  
10 National Key R&D Program ("Developmental Programming and Its  
11 Metabolic Regulation" 2018YFA0801000).

12

13

14

## 15 **References**

16 [1] E. Perspicace, V. Jouan-Hureaux, R. Ragno, F. Ballante, S. Sartini, C  
17 La Motta, F. Da Settimo, B Chen, G Kirsch, S. Hesse, Design, synthesis  
18 and biological evaluation of new classes of thieno[3,2-d]pyrimidinone  
19 and thieno[1,2,3]triazine as inhibitor of vascular endothelial growth factor  
20 receptor-2 (VEGFR-2), Eur. J. Med. Chem. 63 (2013) 765-781.

21 [2] T. Jiang, J. Zhuang, H. Duan, Y. Luo, Q. Zeng, K. Fan, H. Yan, D. Lu,  
22 Z. Ye, J. Hao, J. Feng, D. Yang, X. Yan, CD146 is a coreceptor for

- 1 VEGFR-2 in tumor angiogenesis, *Blood*. 120 (2012) 2330-2339.
- 2 [3] H. K. Mahmoud, T. A. Farghaly, H. G. Abdulwahab, N. T. Al-Qurashi,  
3 M. R. Shaaban, Novel 2-indolinone thiazole hybrids as sunitinib  
4 analogues: Design, synthesis, and potent VEGFR-2 inhibition with  
5 potential anti-renal cancer activity, *Eur. J. Med. Chem.* 208 (2020)  
6 112752.
- 7 [4] S. Sana, V. G. Reddy, S. Bhandari, T. S. Reddy, R. Tokala, A. P. Sakla,  
8 S. K. Bhargava, N. Shankaraiah, Exploration of carbamide derived  
9 pyrimidine-thioindole conjugates as potential VEGFR-2 inhibitors with  
10 anti-angiogenesis effect, *Eur. J. Med. Chem.* 200 (2020) 112457.
- 11 [5] P. M. Hoff, K. K. Machado, Role of angiogenesis in the pathogenesis  
12 of cancer, *Cancer Treat. Rev.* 38 (2012) 825–833.
- 13 [6] P. Carmeliet, R. K. Jain, Molecular mechanisms and clinical  
14 applications of angiogenesis, *Nature*. 473 (2011) 298-307.
- 15 [7] C. Fontanella, E. Ongaro, S. Bolzonello, M. Guardascione, G. Fasola,  
16 G. Aprile, Clinical advances in the development of novel VEGFR-2  
17 inhibitors, *Ann. Transl. Med.* 2 (2014) 123-132.
- 18 [8] G. M. Saidel, Quantitative Relationships of Intravascular Tumor Cells,  
19 Tumor Vessels, and Pulmonary Metastases following Tumor Implantation,  
20 *Cancer Res.* 34 (1974) 997-1004.
- 21 [9] J. Folkman, Angiogenesis: An organizing principle for drug  
22 discovery?, *Nat. Rev. Drug Discov.* 6 (2007) 273–286.

- 1 [10] D. Hanahan, R. A. Weinberg, Hallmarks of cancer: The next  
2 generation, *Cell*. 144 (2011) 646-674.
- 3 [11] J. Q. Wu, R. Y. Fan, S. R. Zhang, C. Y. Li, L. Z. Shen, P. Wei, Z. H.  
4 He, M. F. He, A systematical comparison of anti-angiogenesis and  
5 anti-cancer efficacy of ramucirumab, apatinib, regorafenib and  
6 cabozantinib in zebrafish model, *Life Sci*. 247 (2020) 117402.
- 7 [12] S. M. Chang, V Jain, T. L. Chen, A. S. Patel, H. B. Pidugu, Y. W. Lin,  
8 M. H. Wu, J. R. Huang, H. C. Wu, A. Shah, T. L. Su, T. C. Lee, Design  
9 and Synthesis of 1, 2-Bis (hydroxymethyl)pyrrolo[2,1- a]phthalazine  
10 Hybrids as Potent Anticancer Agents that Inhibit Angiogenesis and  
11 Induce DNA Interstrand Cross-links, *J. Med. Chem*, 62 (2019)  
12 2404-2418.
- 13 [13] H. A. Mahdy, M. K. Ibrahim, A. M. Metwaly, A. Belal, A. B. M.  
14 Mehany, K. M. A. El-Gamal, A. El-Sharkawy, M. A. Elhendawy, M. M.  
15 Radwan, M. A. Elsohly, I. H. Eissa, Design, synthesis, molecular  
16 modeling, in vivo studies and anticancer evaluation of  
17 quinazolin-4(3H)-one derivatives as potential VEGFR-2 inhibitors and  
18 apoptosis inducers. *Bioorg Chem*. 94 (2020) 103422.
- 19 [14] H. T. Abdel-Mohsen, M. A. Omar, A. M. El Kerdawy, A. E. E.  
20 Mahmoud, M. M. Ali, H. I. El Diwani, Novel potent substituted  
21 4-amino-2-thiopyrimidines as dual VEGFR-2 and BRAF kinase inhibitors,  
22 *Eur. J. Med. Chem*. 179 (2019) 707–722.

- [15] D. H. Dawood, E. S. Nossier, M. M. Ali, A. E. Mahmoud, Synthesis and molecular docking study of new pyrazole derivatives as potent anti-breast cancer agents targeting VEGFR-2 kinase, *Bioorg. Chem.* 101 (2020).
- [16] L. Shi, J. Zhou, J. Wu, Y. Shen, X. Li, Anti-Angiogenesis Therapy: Strategies to Develop Potent VEGFR-2 Tyrosine Kinase Inhibitors and Future Prospect, *Curr. Med. Chem.* 23 (2016) 1000-1040.
- [17] S. Faivre, G. Demetri, W. Sargent, E. Raymond, Molecular basis for sunitinib efficacy and future clinical development, *Nat. Rev. Drug Discov.* 6 (2007) 734-745.
- [18] F. Koinis, P. Corn, N. Parikh, J. Song, I. Vardaki, I. Mourkioti, S. H. Lin, C. Logothetis, T. Panaretakis, G. Gallick, Resistance to MET/VEGFR2 inhibition by cabozantinib is mediated by YAP/TBX5-dependent induction of FGFR1 in castration-resistant prostate cancer, *Cancers (Basel)*. 12 (2020) 244.
- [19] V. G. Reddy, T. S. Reddy, C. Jadala, M. S. Reddy, F. Sultana, R. Akunuri, S. K. Bhargava, D. Wlodkowic, P. Srihari, A. Kamal, Pyrazolo-benzothiazole hybrids: Synthesis, anticancer properties and evaluation of antiangiogenesis activity using in vitro VEGFR-2 kinase and in vivo transgenic zebrafish model, *Eur. J. Med. Chem.* 182 (2019) 111609.
- [20] S. Mohamady, M. Galal, W. M. Eldehna, D. C. Gutierrez, H. S.

- 1 Ibrahim, M. M. Elmazar, H. I. Ali, Dual Targeting of VEGFR2 and C-Met  
2 Kinases via the Design and Synthesis of Substituted  
3 3-(Triazolo-thiadiazin-3-yl)indolin-2-one Derivatives as Angiogenesis  
4 Inhibitors, ACS Omega. 5 (2020) 18872-18886.
- 5 [21] H. M. Roaiah, I. A. Y. Ghannam, I. H. Ali, A. M. El Kerdawy, M. M.  
6 Ali, S. E. S. Abbas, S. S. El-Nakkady, Design, synthesis, and molecular  
7 docking of novel indole scaffold-based VEGFR-2 inhibitors as targeted  
8 anticancer agents, Arch. Pharm. 351 (2018) 1-17.
- 9 [22] B. Beuselinck, S. Oudard, O. Rixe, P. Wolter, A. Blesius, J. Ayllon, R.  
10 Elaidi, P. Schöffski, E. Barrascout, A. Morel, B. Escudier, H. Lang, J.  
11 Zucman-Rossi, J. Medioni, Negative impact of bone metastasis on  
12 outcome in clear-cell renal cell carcinoma treated with sunitinib, Ann.  
13 Oncol.22 (2011)794-800.
- 14 [23] P. C. Tang, Y. D. Su, J. Feng, J. H. Fu, J. L. Yang, L. Xiao, J. H. Peng,  
15 Y. L. Li, L. Zhang, B. Hu, Y. Zhou, F. Q. Li, B. B. Fu, L. G. Lou, A. S.  
16 Gong, G. H. She, W. H. Sun, X. T. Mong, Novel potent orally active  
17 multitargeted receptor tyrosine kinase inhibitors: Synthesis,  
18 structure-activity relationships, and antitumor activities of 2-indolinone  
19 derivatives, J. Med. Chem. 53 (2010) 8140-8149.
- 20 [24] H. E. Dweedar, H. Mahrous, H. S. Ibrahim, H. A. Abdel-Aziz,  
21 Analogue-based design, synthesis and biological evaluation of  
22 3-substituted-(methylenedrazono)indolin-2-ones as anticancer agents,

- 1 Eur. J. Med. Chem. 78 (2014) 275-280.
- 2 [25] M. Qin, Y. Tian, X. Han, Q. Cao, S. Zheng, C. Liu, X. Wu, L. Liu, Y.  
3 Meng, X. Wang, H. Zhang, Y. Hou, Structural modifications of  
4 indolinones bearing a pyrrole moiety and discovery of a multi-kinase  
5 inhibitor with potent antitumor activity, Bioorganic Med. Chem. 28 (2020)  
6 115486.
- 7 [26] L. Zhang, Q. Zheng, Y. Yang, H. Zhou, X. Gong, S. Zhao, C. Fan,  
8 Synthesis and in vivo SAR study of indolin-2-one-based multi-targeted  
9 inhibitors as potential anticancer agents, Eur. J. Med. Chem. 82 (2014)  
10 139-151.
- 11 [27] A. M. S. El-Sharief, Y. A. Ammar, A. Belal, M. A. M. S. El-Sharief,  
12 Y. A. Mohamed, A. B. M. Mehany, G. A. M. Elhag Ali, A. Ragab, Design,  
13 synthesis, molecular docking and biological activity evaluation of some  
14 novel indole derivatives as potent anticancer active agents and apoptosis  
15 inducers, Bioorg. Chem. 85 (2019) 399-412.
- 16 [28] J. Guo, F. Zhao, W. Yin, M. Zhu, C. Hao, Y. Pang, T. Wu, J. Wang, D.  
17 Zhao, H. Li, M. Cheng, Design, synthesis, structure-activity relationships  
18 study and X-ray crystallography of  
19 3-substituted-indolin-2-one-5-carboxamide derivatives as PAK4  
20 inhibitors, Eur. J. Med. Chem. 155 (2018) 197-209.
- 21 [29] D. Wu, A. Pusuluri, D. Vogus, V. Krishnan, C. W. Shields, J. Kim, A.  
22 Razmi, S. Mitragotri, Design principles of drug combinations for

- 1 chemotherapy, *J. Control. Release.* 323 (2020) 36-46.
- 2 [30] J. J. Yang, W. W. Yu, L. L. Hu, W. J. Liu, X. H. Lin, W. Wang, Q.  
3 Zhang, P. L. Wang, S. W. Tang, X. Wang, M. Liu, W. Lu, H. K. Zhang,  
4 Discovery and Characterization of 1 H-1,2,3-Triazole Derivatives as  
5 Novel Prostanoid EP4 Receptor Antagonists for Cancer Immunotherapy, *J.*  
6 *Med. Chem.* 63 (2020) 569–590.
- 7 [31] M. Taddei, S. Ferrini, L. Giannotti, M. Corsi, F. Manetti, G. Giannini,  
8 L. Vesci, F. M. Milazzo, D. Alloatti, M. B. Guglielmi, M. Castorina, M. L.  
9 Cervoni, M. Barbarino, R. Foderà, V. Carollo, C. Pisano, S. Armaroli, W.  
10 Cabri, Synthesis and evaluation of new Hsp90 inhibitors based on a  
11 1,4,5-trisubstituted 1,2,3-triazole scaffold, *J. Med. Chem.* 57 (2014)  
12 2258–2274.
- 13 [32] Z. Xu, S. J. Zhao, Y. Liu, 1,2,3-Triazole-containing hybrids as  
14 potential anticancer agents: Current developments, action mechanisms  
15 and structure-activity relationships, *Eur. J. Med. Chem.* 183 (2019)  
16 111700.
- 17 [33] S. Li, X. Y. Li, T. J. Zhang, M. O. Kamara, J. W. Liang, J. Zhu, F. H.  
18 Meng, Design, synthesis and biological evaluation of homoerythrina  
19 alkaloid derivatives bearing a triazole moiety as PARP-1 inhibitors and as  
20 potential antitumor drugs, *Bioorg. Chem.* 94 (2020) 103385.
- 21 [34] G. Q. Lu, X. Y. Li, M. O. Kamara, D. Wang, F. hao Meng, Design,  
22 synthesis and biological evaluation of novel uracil derivatives bearing



- 1 1,2,3-triazole moiety as thymidylate synthase (TS) inhibitors and as  
2 potential antitumor drugs, *Eur. J. Med. Chem.* 171 (2019) 282-296.
- 3 [35] S. Li, X. Y. Li, T. J. Zhang, J. Zhu, W. H. Xue, X. H. Qian, F. H.  
4 Meng, Design, synthesis and biological evaluation of erythrina  
5 derivatives bearing a 1,2,3-triazole moiety as PARP-1 inhibitors, *Bioorg.*  
6 *Chem.* 96 (2020) 103575.
- 7 [36] A. Kamal, S. Prabhakar, M. J. Ramaiah, P. V. Reddy, C. R. Reddy, A.  
8 Mallareddy, N. Shankaraiah, T. L. N. Reddy, S. N. C. V. L. Pushpavalli,  
9 M. Pal-Bhadra, Synthesis and anticancer activity of  
10 chalcone-pyrrolobenzodiazepine conjugates linked via 1,2,3-triazole ring  
11 side-armed with alkane spacers, *Eur. J. Med. Chem.* 46 (2011) 3820–  
12 3831.
- 13 [37] Q. Zhang, Y. Teng, Y. Yuan, T. Ruan, Q. Wang, X. Gao, Y. Zhou, K.  
14 Han, P. Yu, K. Lu, Synthesis and cytotoxic studies of novel 5-phenylisatin  
15 derivatives and their anti-migration and anti-angiogenesis evaluation, *Eur.*  
16 *J. Med. Chem.* 156 (2018) 800–814.
- 17 [38] N. Kaila, K. Janz, A. Huang, A. Moretto, S. Debernardo, P. W.  
18 Bedard, S. Tam, V. Clerin, J. C Keith, D. H. H. Tsao,  
19 2-(4-Chlorobenzyl)-3-hydroxy-7,8,9,10-tetrahydrobenzo[H]quinoline-4-c  
20 arboxylic acid (PSI-697): identification of a clinical candidate from the  
21 quinoline salicylic acid series of P-selectin antagonists, *J. Med. Chem.* 50  
22 (2007) 40-64.

- [39] N. A. Lozinskaya, D. A. Babkov, E. V. Zaryanova, E. N. Bezsonova, A. M. Efremov, M. D. Tsymlyakov, L. V. Anikina, O. Y. Zakharyascheva, A. V. Borisov, V. N. Perfilova, I. N. Tyurenkov, M. V. Proskurnina, A. A. Spasov, Synthesis and biological evaluation of 3-substituted 2-oxindole derivatives as new glycogen synthase kinase 3 $\beta$  inhibitors, *Bioorganic Med. Chem.* 27 (2019) 1804–1817.
- [40] Y. Z. Zhou, Y. Ju, Y. Yang, Z. Sang, Z. Wang, G. He, T. Yang, Y. Luo, Discovery of hybrids of indolin-2-one and nitroimidazole as potent inhibitors against drug-resistant bacteria, *J. Antibiot.* 71 (2018) 887–897.
- [41] W. D. Long, W. L. Ying, W. Y. Ling, S. Shuang, F. J. Tao, Z. Xing, Natural  $\alpha$ -methylenelactam analogues: Design, synthesis and evaluation of  $\alpha$ -alkenyl- $\gamma$  and  $\delta$ -lactams as potential antifungal agents against *Colletotrichum orbiculare*, *Eur. J. Med. Chem.* 130 (2017) 286–307.
- [42] M. E. Matheus, F. de A. Violante, S. J. Garden, A. C. Pinto, P. D. Fernandes, Isatins inhibit cyclooxygenase-2 and inducible nitric oxide synthase in a mouse macrophage cell line, *Eur. J. Pharmacol.* 556 (2007) 200–206.
- [43] B. R. Dinesh, A. R. Baba, K. U. Sankar, D. C. Gowda, Synthesis of indolones and quinolones by reductive cyclisation of o-nitroaryl acids using zinc dust and ammonium formate, *J. Chem. Res.* (2008) 287–288.
- [44] S. Shah, C. Lee, H. Choi, J. Gautam, H. Jang, G. J. Kim, Y. J. Lee, C. L. Chaudhary, S.W. Park, T. G. Nam, J. A. Kim, B. S. Jeong,

- 1 5-Hydroxy-7-azaindolin-2-one, a novel hybrid of pyridinol and sunitinib:  
2 Design, synthesis and cytotoxicity against cancer cells, *Org. Biomol.*  
3 *Chem.* 14 (2016) 4829–4841.
- 4 [45] L. Sun, N. Tran, F. Tang, H. App, P. Hirth, G. McMahon, C. Tang,  
5 Synthesis and biological evaluations of 3-substituted indolin-2-ones: A  
6 novel class of tyrosine kinase inhibitors that exhibit selectivity toward  
7 particular receptor tyrosine kinases, *J. Med. Chem.* 41 (1998) 2588–2603.
- 8 [46] H. Yang, C. Lou, L. Sun, J. Li, Y. Cai, Z. Wang, W. Li, G. Liu, Y.  
9 Tang, AdmetSAR 2.0: Web-service for prediction and optimization of  
10 chemical ADMET properties, *Bioinformatics.* 35 (2019) 1067–1069.
- 11 [47] X. yang Li, S. Li, G. qing Lu, D. pu Wang, K. li Liu, X. hua Qian, W.  
12 han Xue, F. hao Meng, Design, synthesis and biological evaluation of  
13 novel (E)-N-phenyl-4-(pyridine-acylhydrazone) benzamide derivatives as  
14 potential antitumor agents for the treatment of multiple myeloma (MM),  
15 *Bioorg. Chem.* 103 (2020) 104189.
- 16 [48] Z. Gao, M. Shi, Y. Wang, J. Chen, Y. Ou, Apatinib enhanced  
17 anti-tumor activity of cisplatin on triple-negative breast cancer through  
18 inhibition of VEGFR-2, *Pathol. Res. Pract.* 215 (2019) 152422.
- 19 [49] X. Y. Li, T. J. Zhang, M. O. Kamara, G. Q. Lu, H. L. Xu, D. P. Wang,  
20 F. H. Meng, Discovery of  
21 N-phenyl-(2,4-dihydroxypyrimidine-5-sulfonamido) phenylurea-based  
22 thymidylate synthase (TS) inhibitor as a novel multi-effects antitumor

- 1 drugs with minimal toxicity, *Cell Death Dis.* 10 (2019) 532.
- 2 [50] J. L. Velázquez-Libera, J. Caballero, J. A. Murillo-López, A. F. de la  
3 Torre, Structural requirements of n-alpha-mercaptoacetyl dipeptide  
4 (Namdp) inhibitors of *pseudomonas aeruginosa* virulence factor lasb:  
5 3Q-QSAR, molecular docking, and interaction fingerprint studies, *Int. J.*  
6 *Mol. Sci.* 20 (2019) 6133.
- 7 [51] M. McTigue, B. W. Murray, J. H. Chen, Y. L. Deng, J. Solowiej, R. S.  
8 Kania,. Molecular conformations, interactions, and properties associated  
9 with drug efficiency and clinical performance among VEGFR TK  
10 inhibitors, *P. Natl. Acad. Sci. USA.* 109 (2012) 18281–18289.
- 11 [52] T. J Zhang, Y. Zhang, S. Tu, Y. H. Wu , Z. H. Zhang, F. H. Meng,  
12 Design, synthesis and biological evaluation of  
13 N-(3-(1H-tetrazol-1-yl)phenyl)isonicotinamide derivatives as novel  
14 xanthine oxidase inhibitors, *Eur. J. Med. Chem.* 183 (2019) 111717.

15

- A novel VEGFR-2 inhibitor based on 1,2,3-triazole scaffold was identified.
- Compound **13d** had better kinase activity inhibition ability than sunitinib.
- Compound **13d** could inhibit angiogenesis more effectively than sunitinib.

## Conflict of Interest

The authors declared that they have no conflicts of interest in this work.

We declared that we do not have any commercial or associative interest that represents a conflict of interest in connection with the work submitted.